

FRACTIONAL GRAVITY AND MODIFIED NEWTONIAN DYNAMICS

Gabriele U. Varieschi*

Loyola Marymount University, Los Angeles, CA 90045, USA

(Dated: May 3, 2022)

This paper introduces a possible alternative model of gravity based on fractional calculus and its applications to Newtonian gravity. In particular, Gauss's law for gravity as well as Laplace's equation and other fundamental classical laws are extended to a D -dimensional metric space, where D can be a non-integer dimension.

We show a possible connection between this Newtonian Fractional Gravity (NFG) and Modified Newtonian Dynamics (MOND), the leading alternative gravity model, which accounts for the observed properties of galaxies and other astrophysical structures without requiring the dark matter hypothesis. The MOND acceleration constant $a_0 \simeq 1.2 \times 10^{-10} \text{ m s}^{-2}$ can be related to a natural scale length l_0 in NFG, i.e., $a_0 \approx GM/l_0^2$, for astrophysical structures of mass M , and the deep-MOND regime is present in regions of space where the dimension is reduced to $D \approx 2$.

For several fundamental spherically-symmetric structures, we compare MOND results such as the empirical Radial Acceleration Relation (RAR), circular speed plots, and logarithmic plots of the observed radial acceleration g_{obs} vs. the baryonic radial acceleration g_{bar} , showing that NFG is capable of reproducing these results using a variable local dimension $D(w)$, where $w = r/l_0$ is a dimensionless radial coordinate. At the moment, we are unable to derive explicitly this dimension function $D(w)$ from first principles, but it can be obtained empirically in each case from the general RAR.

Additional work on the subject, including studies of axially-symmetric structures, detailed galactic rotation curves fitting, and a possible relativistic extension, will be needed to establish NFG as a viable alternative model of gravity.

PACS numbers: 04.50.Kd, 95.30.Sf, 95.35.+d, 98.62.Dm

Keywords: fractional gravity; modified gravity; dark matter; galaxies

* E-mail me at: gvarieschi@lmu.edu ; Visit: <http://gvarieschi.lmu.build>

I. INTRODUCTION

This paper considers a possible generalization of the gravitational Gauss's law and of the other standard laws of Newtonian gravity to lower dimensional cases, including fractional (i.e., non-integer) dimensions. This analysis is based on the application of fractional calculus (FC) [1–5] and fractional mechanics [6, 7] to the classical laws of gravity. Fractional calculus is also commonly related to fractal geometries, which might be relevant at galactic or cosmological scales in the universe [8, 9]. A generalized “Newtonian Fractional Gravity” (NFG) can be derived from the aforementioned principles.

This analysis also shows a possible connection with Modified Newtonian Dynamics (MOND) [10–12], the leading alternative gravity model, originally introduced in 1983 as a possible solution to the mass-discrepancy/dark matter (DM) problem, and later evolved into a relativistic theory [13, 14]. Recently, a strong correlation between the radial gravitational acceleration traced by galactic rotation curves and that predicted by the observed distribution of baryons has been reported [15, 16], consistent with MOND galactic dynamics. In this paper, we propose a possible explanation of this correlation based on a “variable-dimension” effect in galactic structures, thus connecting MOND with Newtonian fractional gravity.

In Sect. II, we describe in more details the original MOND model and the related correlation between observed and baryonic galactic rotational accelerations. In Sect. III, we introduce the fractional generalization of Gauss's law and Newtonian gravity. In Sect. IV, we show applications of these methods to some basic spherical models and establish a connection with the MOND theory. Finally, in Sect. V conclusions are drawn and possible future work on the subject is outlined.

II. MOND AND GALACTIC ROTATION CURVES

Modified Newtonian Dynamics was created in 1982 by Milgrom and first published in 1983 [10–12] as a possible solution to the mass discrepancy problem in galaxies, galaxy systems, and other stellar systems. The original proposal called for a modification of Newtonian dynamics in terms of inertia or gravity, in order to describe the motion of bodies in the gravitational field of a galaxy, or a cluster of galaxies, without the need of any hidden mass, i.e., without any DM contribution. At the core of the MOND model is an acceleration constant a_0 , whose currently estimated value is [15, 16]:

$$a_0 \equiv g_{\dagger} = 1.20 \pm 0.02 \text{ (random)} \pm 0.24 \text{ (syst)} \times 10^{-10} \text{ ms}^{-2} \quad (1)$$

and which represents the acceleration scale below which MOND corrections are applied.¹

The modification to Newtonian dynamics can be expressed in two possible forms [17]:

$$\begin{aligned} m\mu(a/a_0)\mathbf{a} &= \mathbf{F} \\ \mu(g/a_0)\mathbf{g} &= \mathbf{g}_N, \end{aligned} \quad (2)$$

where the former indicates a modification to the law of inertia (Newton's second law): \mathbf{F} is an arbitrary static force and m is the (gravitational) mass of the accelerated test particle. For the force of gravity, $\mathbf{F} = mg_N$, where $\mathbf{g}_N = -\nabla\phi_N$ and ϕ_N is the usual Newtonian gravitational potential derived from the standard Poisson equation. Therefore, this first form of modified dynamics applies to any type of force and changes the law of inertia, since the acceleration \mathbf{a} is replaced by $\mu(a/a_0)\mathbf{a}$.

On the contrary, the second line in Eq. (2) modifies just the gravitational field \mathbf{g} , obtained from the Newtonian \mathbf{g}_N , while leaving the law of inertia ($ma = \mathbf{F}$) unchanged. The two formulations are practically equivalent, but conceptually different: the former modifies Newton's laws of motion, while the latter modifies Newton's law of universal gravitation. In both cases, the modification follows from the *interpolation function* $\mu(x) \equiv \mu(a/a_0)$ or $\mu(x) \equiv \mu(g/a_0)$, respectively.

MOND postulates that:

$$\mu(x) \approx \begin{cases} 1 & \text{for } x \gg 1 \text{ (Newtonian regime),} \\ x & \text{for } x \ll 1 \text{ (deep-MOND regime).} \end{cases} \quad (3)$$

¹ In the latest papers in the literature (such as [15, 16]), this acceleration scale constant is indicated as g_{\dagger} , when derived by fitting galactic data with an empirical law. See Eq. (6) later in this section.

Originally, Milgrom used simple forms for the interpolation function, such as the “standard” form $\mu_2(x) = x/\sqrt{1+x^2}$ or $\mu(x) = 1 - e^{-x}$ [11, 18], while recently other forms have become more popular, such as the “simple” interpolation function $\mu_1(x) = x/(1+x)$, or the general family of functions $\mu_n(x) = x(1+x^n)^{-1/n}$, of which μ_1 and μ_2 are special cases. Also, following the second line in Eq. (2), it has become customary [19] to invert this relation into the following:

$$\mathbf{g} = \mu^{-1}(x)\mathbf{g}_N \equiv \nu(y)\mathbf{g}_N \text{ with } y = g_N/a_0. \quad (4)$$

Several $\nu(y)$ functions were introduced in the literature over the years (see Ref. [19] for full details), but we will consider in the following two main families:

$$\begin{aligned} \nu_n(y) &= \left(\frac{1}{2} + \frac{1}{2} \sqrt{1 + 4y^{-n}} \right)^{1/n}, \\ \widehat{\nu}_n(y) &= \left[1 - \exp \left(-y^{n/2} \right) \right]^{-1/n}. \end{aligned} \quad (5)$$

The first family in the last equation is the inverse of the family $\mu_n(x)$ described above, while the second one corresponds to interpolation functions which are similar to the “simple” function on galaxy scales ($\sim a_0$) while having no impact in the inner solar system ($\sim 10^8 a_0$) [19]. Due to the exponential function in their definition, the functions $\widehat{\nu}_n(y)$ cannot be easily inverted into corresponding $\widehat{\mu}_n(x)$ functions, but the particular choice $\widehat{\nu}_1(y) = [1 - \exp(-y^{1/2})]^{-1}$ has recently become the favorite interpolation function [15, 16].

Continuing our brief historical outline of MOND (see Refs. [20–22] for general reviews), in order to ensure standard conservation laws Milgrom and Bekenstein introduced an Aquadratic Lagrangian theory (AQUAL) [17], in the context of MOND as modified gravity. This was based on a Lagrangian function which generalized the Newtonian one and on a modified Poisson equation, $\nabla \cdot [\mu(|\nabla\phi|/a_0)\nabla\phi] = 4\pi G\rho$, from which the original MOND relation in the second line of Eq. (2) would follow in cases of high symmetry (spherical, cylindrical, or plane).

This version of MOND was then interpreted by Milgrom [23, 24] as an effective theory due to vacuum effects of cosmological origin. This view was also supported by the numerical coincidences: $a_0 \approx cH_0$ and $a_0 \approx c^2\Lambda^{1/2}$, linking the MOND acceleration a_0 with the Hubble constant H_0 and the cosmological constant Λ . The AQUAL model then evolved into different relativistic versions, such as RAQUAL and phase-coupled gravity–PCG [21], which were eventually replaced by other relativistic MOND theories (Tensor–Vector–Scalar theories [13, 14]). Since our analysis will be confined to non-relativistic effects, there is no need to introduce further elements of relativistic MOND.

Back to the non-relativistic model, the main successes of MOND are well-known. In the spirit of “Keplerian” laws, they can be summarized as the three laws of rotationally-supported galaxies (from Ref. [25]):

1. Rotation curves attain an approximately constant velocity (asymptotic or flat rotation velocity V_f) that persists indefinitely (flat rotation curves).
2. The observed baryonic mass scales as the fourth power of the amplitude of the flat rotation curve (the “baryonic” Tully-Fisher relation–BTFR: $M_{bar} \sim V_f^4$).
3. There is a one-to-one correspondence between the radial force and the observed distribution of baryonic matter (the mass discrepancy-acceleration relation $M_{tot}/M_{bar} \simeq V_{obs}^2/V_{bar}^2$).

The first point is the main original MOND prediction from Eqs. (2) and (3), regardless of the chosen interpolation function [11]: at large galactic radii (deep-MOND regime) we can replace $g_N \approx GM/r^2$ and $a = g = V^2/r$ in those two equations and obtain $V^4(r) \equiv V_f^4 \approx GMa_0$, from which $V_f \approx \sqrt[4]{GMa_0}$, where M is the total mass of the galaxy. This initial consideration then evolved into detailed fitting of galactic rotation curves of different shapes without using dark matter (see Refs. [19, 21, 25] for some examples) and firmly established MOND as an alternative to the DM hypothesis.

The second point follows directly from the previous arguments, in particular from $V_f^4 \approx GMa_0$, and from the observed strong correlation (Tully-Fisher relation [26–28]) between galactic total luminosity L and typical rotational velocity V_f : $L \propto V_f^\alpha$ with $\alpha \sim 4$, and by assuming also that the total galactic luminosity is simply proportional to the total mass M . This connection between light and matter is also manifest in more subtle ways: features in galactic luminosity profiles usually correspond to features in the rotation curves and vice-versa (the so-called *Renzo’s rule* [29]).

The third point has recently evolved into a very precise statement relating the radial acceleration g_{obs} traced by rotation curves with the radial acceleration g_{bar} predicted by the observed distribution of baryonic matter [15, 16].

Using astrophysical data from the Spitzer Photometry and Accurate Rotation Curves (SPARC) database [30], a sample of 175 galaxies with new photometry and high-quality rotation curves, McGaugh and collaborators were able to produce an empirical fit to all the data points (radial acceleration relation - RAR) as follows:

$$g_{obs} = \frac{g_{bar}}{1 - e^{-\sqrt{g_{bar}/g_{\dagger}}}}, \quad (6)$$

where g_{\dagger} is an empirical acceleration parameter, corresponding to the MOND (theoretical) acceleration scale a_0 , whose value we already reported in Eq. (1) above. While Eq. (6) represents a pure empirical fit, in spirit similar to Kepler's third law, it can be noted immediately that it corresponds to one of the MOND interpolation functions described above, namely, the particular function $\hat{\nu}_1(y) = [1 - \exp(-y^{1/2})]^{-1}$, once we identify $y = g_N/a_0 \equiv g_{bar}/g_{\dagger}$ and $\hat{\nu}_1 = g/g_N \equiv g_{obs}/g_{bar}$.

It should be also noted that the above fit involved 2693 data points from 153 rotationally supported (spiral and irregular) galaxies [15], spanning over a large range of physical properties, such as rotation velocities, luminosities, effective surface brightness, etc. The baryonic acceleration g_{bar} was computed first by solving numerically the standard Poisson equation $\nabla^2 \phi_{bar} = 4\pi G \rho_{bar}$, with the baryonic mass density ρ_{bar} obtained from near-infrared (3.6 μ m) data tracing the stellar mass distribution and from 21cm hydrogen line data tracing the atomic gas, and then by deriving g_{bar} from the gravitational potential: $g_{bar} = |\frac{\partial \phi_{bar}}{\partial R}|$. The observed acceleration g_{obs} was obtained directly from the rotation curves as $g_{obs} = V^2/R$. By using a single value for the stellar mass-to-light ratio $\Upsilon_*^{[3.6]} = 0.50 M_{\odot}/L_{\odot}$ [15], the fit in Eq. (6) provides a universal empirical equation based just on the MOND parameter $g_{\dagger} \equiv a_0$: in Fig. 3 of Ref. [15] nearly 2700 data points are fitted by the RAR and individual galaxies are indistinguishable in that analysis. In Sects. III and IV we will provide a possible explanation of this fundamental empirical relation using NFG.

In more recent work [16], from the original SPARC database of late-type-galaxies (spiral and irregular), the galaxy sample was extended to include early-type-galaxies (elliptical and lenticular) and dwarf spheroidal galaxies, confirming the RAR and, as a consequence, also other dynamical properties of galaxies, like the Tully-Fisher and Faber-Jackson relations, the “baryon-halo” conspiracies, and Renzo's rule. Also, in Ref. [31] the 175 galaxies in the SPARC database were checked individually against the RAR, allowing for galaxy-to-galaxy variations of the acceleration scale g_{\dagger} . The result of this analysis favored a single value of g_{\dagger} , consistent with the action of a single effective force law.

Several other experimental observations are explained by MOND and related relativistic versions (see [22] for a complete discussion), but it should be noted that MOND and its generalizations do not adequately explain properties of galaxy clusters, globular clusters, etc., and are not particularly suited to form the basis of a cosmological model [22]. With respect to these issues and as a standard cosmological model, the Λ CDM concordance model [32] is still the favorite, most successful, cosmological theory.

III. FRACTIONAL GAUSS'S LAW AND NEWTONIAN GRAVITY

An interesting pedagogical problem is the analysis of classical theories, such as Maxwell's electrodynamics or Newtonian gravity, in a lower-dimensional space-time. Rather than using standard $3+1$ space-time, we can decrease the spatial dimension and consider these classical theories in $2+1$, or even $1+1$ space-times. Standard textbooks do not usually discuss these cases, and very few papers (see [33, 34] and references therein) are available in the literature. The study of the laws of physics for cases of dimension $D \neq 3$ was also used at times as a “proof” of the tri-dimensionality of space (see the original analysis by Ehrenfest in 1920 [35] and the more philosophical discussion in Ref. [36]).

Typically, only Maxwell's electrodynamics in lower-dimensional spaces is discussed in the literature [33, 34], but results for electrostatics can be easily adapted to Newtonian gravity. The main issue is whether Coulomb's law should be altered in a lower-dimensional space situation, or remain the usual inverse-square law. This crucial point was clarified by Lapidus [37, 38], who argued that Gauss's law in a two-dimensional space implies an inverse-linear Coulomb's law and thus a logarithmic potential, while in a one-dimensional space the electric field is constant in magnitude and the potential linear. These electrostatic potentials were then used to study one and two-dimensional hydrogen atoms [39, 40].

In the following, we will start from the analysis of electrostatics in two spatial dimensions outlined in Ref. [33] and in the unpublished Ref. [34], adapt it to the gravitational case and then generalize it to an arbitrary fractional dimension D . The laws of electrostatics are easily converted into equivalent gravitational laws by replacing $1/\epsilon_0$ with $-4\pi G$, where ϵ_0 is the permittivity of free space and G is the standard gravitational constant.² In this way, standard

² SI units will be used throughout this paper, unless otherwise noted.

Gauss's law for the electric field \mathbf{E} of a point charge q , placed at the origin in a three-dimensional ($D = 3$) space, describes the (outward) flux of \mathbf{E} through a spherical surface S of radius r as: $\Phi_E^{(3)} = |\mathbf{E}| r^2 \int_S d\Omega = |\mathbf{E}| 4\pi r^2 = q/\epsilon_0$.

The equivalent law for the (attractive) gravitational field \mathbf{g} due to a point mass m is:

$$\Phi_g^{(3)} = -|\mathbf{g}| r^2 \int_S d\Omega = -|\mathbf{g}| 4\pi r^2 = -4\pi Gm, \quad (7)$$

which yields the usual inverse-square law for the gravitational field: $|\mathbf{g}| = Gm/r^2$.

Gauss's law can be generalized to any (positive) dimension D by considering a hypersphere S of radius r as a Gaussian surface with $\int_S d\Omega_D = \frac{2\pi^{D/2}}{\Gamma(D/2)}$, which follows from standard dimensional regularization techniques commonly used in quantum field theory (see, for example, [41] page 249, or the original Refs. [42–44]). Similar regularization methods on fractal space-times [6, 7, 45] generalize the integral of a spherically-symmetric function $f = f(r)$ over a fractal D -dimensional metric space W as follows:

$$\int_W f d\mu_H = \frac{2\pi^{D/2}}{\Gamma(D/2)} \int_0^\infty f(r) r^{D-1} dr, \quad (8)$$

where μ_H denotes an appropriate Hausdorff measure over the space.

In fractional calculus,³ the integral on the right-hand side of Eq. (8) is related to the Weyl's fractional integral⁴ defined as $W^{-D} f(x) = \frac{1}{\Gamma(D)} \int_x^\infty (t-x)^{D-1} f(t) dt$, so that Eq. (8) can also be written as [6, 45]:

$$\int_W f d\mu_H = \frac{2\pi^{D/2} \Gamma(D)}{\Gamma(D/2)} W^{-D} f(0). \quad (9)$$

This equation connects the integral over a fractal space W of dimension D with an integral of fractional order up to the numerical factor $2\pi^{D/2} \Gamma(D)/\Gamma(D/2)$, thus establishing a direct relation between fractal space-time and fractional calculus.

In view of this discussion, the generalized gravitational Gauss's law becomes:

$$\Phi_g^{(D)} = -|\mathbf{g}| r^{D-1} \int_S d\Omega_D = -|\mathbf{g}| r^{D-1} \frac{2\pi^{D/2}}{\Gamma(D/2)} = -4\pi Gm_{(D)}, \quad (10)$$

where $m_{(D)}$ represents a “point-mass” in a fractal D -dimensional space. Since $\Gamma(3/2) = \frac{\sqrt{\pi}}{2}$, for $D = 3$ the last equation reduces to the standard law $|\mathbf{g}| = \frac{Gm_{(3)}}{r^2}$, with $m_{(3)} = m$ representing the standard mass measured in kilograms. For $D = 2$ and $D = 1$, we obtain respectively $|\mathbf{g}| = \frac{2Gm_{(2)}}{r}$ and $|\mathbf{g}| = 2\pi Gm_{(1)}$ (since $\Gamma(1) = 0! = 1$ and $\Gamma(1/2) = \sqrt{\pi}$). Assuming that $|\mathbf{g}|$ (in m s^{-2}) and $G = 6.674 \times 10^{-11} \text{m}^3 \text{kg}^{-1} \text{s}^{-2}$ retain the same physical dimensions (and the same value for G) in any D -dimensional space, it is easy to check that $m_{(2)}$ and $m_{(1)}$ will have dimensions of mass per unit length (kg m^{-1}) and mass per unit surface (kg m^{-2}), respectively.

This is consistent with the general idea [34] that electrostatics (or Newtonian gravity) in two spatial dimensions (x, y) should be equivalent to that in three spatial dimensions (x, y, z) for situations in which the 3-dimensional charge (mass) distributions are independent of z , i.e., lines of constant charge (mass) density in the z direction, whose fields scale like the inverse of the distance. Similarly, in one spatial dimension (x) , we should consider as sources surfaces of constant charge (mass) density independent of (y, z) , i.e., surfaces parallel to the (y, z) plane, whose fields are uniform.

From Eq. (10), we can obtain the general expression for the gravitational field as $|\mathbf{g}| = 2\pi^{1-D/2} \Gamma(D/2) \frac{Gm_{(D)}}{r^{D-1}}$, with $m_{(D)}$ measured in kg m^{D-3} . To avoid this awkward unit for masses in D -dimensional spaces, we prefer to redefine the mass as $m_{(D)} = \tilde{m}_{(D)}/l_0^{3-D}$, where l_0 represents a scale length (in meters) and $\tilde{m}_{(D)}$ is now measured in kilograms. Our preferred expression for the gravitational field becomes:

³ For a basic introduction to FC and some elementary physics application see Ref. [46].

⁴ In FC there are several possible definitions of fractional integrals and derivatives and notation also differs in leading textbooks [1–5]. For example, following Ref. [2], the Riemann integral is defined as ${}_c D_x^{-\nu} f(x) = \frac{1}{\Gamma(\nu)} \int_c^x (x-t)^{\nu-1} f(t) dt$, the Liouville integral ($c = -\infty$) as ${}_{-\infty} D_x^{-\nu} f(x) = \frac{1}{\Gamma(\nu)} \int_{-\infty}^x (x-t)^{\nu-1} f(t) dt$, the Riemann-Liouville ($c = 0$) as ${}_0 D_x^{-\nu} f(x) = \frac{1}{\Gamma(\nu)} \int_0^x (x-t)^{\nu-1} f(t) dt$, and the Weyl fractional integral as ${}_x W_{\infty}^{-\nu} f(x) = \frac{1}{\Gamma(\nu)} \int_x^\infty (t-x)^{\nu-1} f(t) dt$. Some textbooks [6] prefer to distinguish between left-sided integrals, such as ${}_c D_x^{-\nu} f(x) = \frac{1}{\Gamma(\nu)} \int_c^x (x-t)^{\nu-1} f(t) dt$, and right-sided integrals, such as ${}_x D_c^{-\nu} f(x) = \frac{1}{\Gamma(\nu)} \int_x^c (t-x)^{\nu-1} f(t) dt$; in this way the Weyl integral is the right-sided version of the left-sided Liouville integral above

$$|\mathbf{g}| = 2\pi^{1-D/2}\Gamma(D/2)\frac{G\tilde{m}_{(D)}}{l_0^2}\frac{1}{(r/l_0)^{D-1}} \approx \frac{Gm_{(3)}}{l_0^2}\frac{1}{(r/l_0)^{D-1}}. \quad (11)$$

In the last equation, we have also assumed that $m \equiv m_{(3)} \approx 2\pi^{1-D/2}\Gamma(D/2)\tilde{m}_{(D)}$ for simplicity's sake. This is consistent with the discussion above that a 3-dimensional mass $m_{(3)}$ should be replaced by $2\tilde{m}_{(2)} = 2m_{(2)}l_0$ in 2-dim, and by $2\pi\tilde{m}_{(1)} = 2\pi m_{(1)}l_0^2$ in 1-dim, where $m_{(2)}$ and $m_{(1)}$ are linear and surface mass densities, respectively. The scale length l_0 in Eq. (11) is still undetermined, but the combination $Gm_{(3)}/l_0^2$ represents a scale acceleration for the field of a point particle $m = m_{(3)}$ in a fractal space of dimension D . It is possible to identify tentatively this scale acceleration with the similar MOND acceleration parameter a_0 :⁵

$$a_0 \approx \frac{Gm_{(3)}}{l_0^2}, \quad (12)$$

and consider the deep-MOND regime as being equivalent to the $D = 2$ case of Eq. (11),

$$|\mathbf{g}|_{deep-MOND} \approx \frac{Gm_{(3)}}{l_0^2}\frac{1}{(r/l_0)} = \frac{a_0 l_0}{r}. \quad (13)$$

This approach is consistent with the MOND analysis of circular motion of a test object in the field generated by a total mass M . As seen in Sect. II, MOND computes the flat (asymptotic) rotational speed V_f as $V_f^4 = GMa_0$, in strong agreement with the baryonic Tully-Fisher relation. Combining our last two equations with $m_{(3)} = M$ and setting $|\mathbf{g}|_{deep-MOND} = V_f^2/r$, as in standard Newtonian dynamics, we obtain the same result $V_f^4 = GMa_0$.

Furthermore, our approach is also consistent with the (simplified) MOND analysis of binary galaxies, considered as point-like masses in circular orbits [12]. Assuming that the binaries contain galaxies of equal mass M , denoting with R the true separation and with V the velocity difference, standard Newtonian gravity computes $V^2 = 2GM/R$, while MOND [12] obtains instead $V^4 = 4a_0GM$. Since the reduced mass of the system is $M/2$, and using Eqs. (12) and (13) with $m_{(3)} = M$, we obtain $\frac{M}{2}\frac{V^2}{R} = M|\mathbf{g}|_{deep-MOND} = \frac{M a_0 l_0}{R}$, from which $V^2 = 2a_0 l_0 = 2a_0 \sqrt{GM/a_0}$ and, by squaring, we obtain the same MOND relation for V^4 as above.

The two simple cases just described also confirm our choice to set $m \equiv m_{(3)} \approx 2\pi^{1-D/2}\Gamma(D/2)\tilde{m}_{(D)}$ for any value of D . For example, a unit mass $m = m_{(3)} = 1$ kg in a three-dimensional space would effectively correspond to $\tilde{m}_{(2)} = \frac{1}{2}$ kg in a two-dimensional space, or to $\tilde{m}_{(1)} = \frac{1}{2\pi}$ kg in a one-dimensional space.⁶

Considering Eq. (11) for an infinitesimal source mass $d\tilde{m}_{(D)}$ and integrating over the D -dimensional source volume V_D :

$$\mathbf{g}(\mathbf{w}) = -\frac{2\pi^{1-D/2}\Gamma(D/2)G}{l_0^2} \int_{V_D} d\tilde{m}_{(D)} \frac{(\mathbf{x} - \mathbf{x}')/l_0}{(|\mathbf{x} - \mathbf{x}'|/l_0)^D} = -\frac{2\pi^{1-D/2}\Gamma(D/2)G}{l_0^2} \int_{V_D} \tilde{\rho}(\mathbf{w}') \frac{\mathbf{w} - \mathbf{w}'}{|\mathbf{w} - \mathbf{w}'|^D} d^D \mathbf{w}', \quad (14)$$

where the source mass $d\tilde{m}_{(D)}$ is described by the position \mathbf{x}' . In this equation, we have also introduced dimensionless coordinates $\mathbf{w} \equiv \mathbf{x}/l_0$ for the field point and $\mathbf{w}' \equiv \mathbf{x}'/l_0$ for the source point. It should be noted that the mass “density” $\tilde{\rho}(\mathbf{w}')$ is actually measured in kilograms, since $d\tilde{m}_{(D)} = \tilde{\rho}(\mathbf{w}') d^D \mathbf{w}'$ (or $\tilde{\rho}(\mathbf{w}') = \rho(\mathbf{w}' l_0) l_0^3 = \rho(\mathbf{x}') l_0^3$, where $\rho(\mathbf{x}')$ is the standard mass density in kg m^{-3}). We will use these dimensionless coordinates \mathbf{w} and \mathbf{w}' in the following, since they are more convenient to describe fractal media and they ensure dimensional correctness of all physical equations.

It should also be noted that in Eq. (14) the space dimension D might be a function of the field point coordinate \mathbf{w} . On the contrary, we considered the scale length l_0 as a constant for the particular source mass distribution being considered. In Sect. IV we will discuss these choices in the context of different possible galactic structures.

The “volume” integral over V_D can be performed by using techniques of multi-variable integration over a fractal metric space $W \subset \mathbb{R}^3$ [6, 7, 47, 48]. Let's assume that $W = W_1 \times W_2 \times W_3$, where each metric set W_i ($i = 1, 2, 3$)

⁵ In the literature [14], the quantity $r_m = \sqrt{GM/a_0}$ is sometimes called the MOND radius. In view of Eq. (12), our fundamental scale length l_0 is equivalent to the MOND radius r_m .

⁶ More generally, it should be noted that we could have defined $a_0 \approx C^2 \frac{Gm_{(3)}}{l_0^2}$, $l_0 \approx C \sqrt{\frac{Gm_{(3)}}{a_0}}$ with $C > 0$ constant. This choice would also yield $V_f^4 = GMa_0$ for the flat rotational speed and $V^4 = 4a_0GM$ for a simple binary system of equal mass M , using our equations with $D = 2$. We have opted to simply set $C = 1$ in Eq. (12), which also justifies the assumption in the right-hand side of Eq. (11).

has Hausdorff measure $\mu_i(W_i)$ and dimension α_i . The Hausdorff measure for the product set W can be defined as $\mu_H(W) = (\mu_1 \times \mu_2 \times \mu_3)(W) = \mu_1(W_1)\mu_2(W_2)\mu_3(W_3)$ and the overall fractal dimension is $D = \alpha_1 + \alpha_2 + \alpha_3$. Applying Fubini's theorem we have:

$$\int_W f(x_1, x_2, x_3) d\mu_H = \int_{W_1} \int_{W_2} \int_{W_3} f(x_1, x_2, x_3) d\mu_1(x_1) d\mu_2(x_2) d\mu_3(x_3), \quad (15)$$

$$d\mu_i(x_i) = \frac{\pi^{\alpha_i/2}}{\Gamma(\alpha_i/2)} |x_i|^{\alpha_i-1} dx_i, \quad i = 1, 2, 3.$$

It is straightforward to check that the integral defined in Eq. (15) when applied to a function $f(x_1, x_2, x_3) = f(r)$, in standard spherical coordinates (r, θ, φ) , yields the expression in Eq. (8). In fact, from the standard relations between rectangular and spherical coordinates and using the definitions for the differentials in the second line of Eq. (15), we have: $d\mu_1 d\mu_2 d\mu_3 = \frac{\pi^{\alpha_1/2}}{\Gamma(\alpha_1/2)} \frac{\pi^{\alpha_2/2}}{\Gamma(\alpha_2/2)} \frac{\pi^{\alpha_3/2}}{\Gamma(\alpha_3/2)} r^{\alpha_1+\alpha_2+\alpha_3-1} dr |\sin \theta|^{\alpha_1+\alpha_2-1} |\cos \theta|^{\alpha_3-1} d\theta |\sin \varphi|^{\alpha_2-1} |\cos \varphi|^{\alpha_1-1} d\varphi$. Performing the angular integrations, simplifying the results, and using $D = \alpha_1 + \alpha_2 + \alpha_3$ leads to the result in Eq. (8).

If we used instead cylindrical coordinates (r, φ, z) with a function $f(x_1, x_2, x_3) = f(r, z)$, we would obtain:

$$\int_W f d\mu_H = \frac{2\pi^{D/2}}{\Gamma[(\alpha_r + \alpha_\varphi)/2]\Gamma(\alpha_z/2)} \int r^{\alpha_r+\alpha_\varphi-1} dr \int f(r, z) |z|^{\alpha_z-1} dz, \quad (16)$$

with $D = \alpha_r + \alpha_\varphi + \alpha_z$.

From Eq. (14), we can also re-derive the original Eq. (11) by using $\tilde{\rho}(\mathbf{w}') = \tilde{m}_{(D)}\delta^{(D)}(\mathbf{w}' - 0)$ where the fractional Dirac delta function is defined as $\int_{V_D} f(\mathbf{w}')\delta^{(D)}(\mathbf{w}' - \mathbf{w})d^D\mathbf{w}' = f(\mathbf{w})$, for any function f over $V_D \subset \mathbb{R}^3$. As in standard Newtonian gravity, it is possible to introduce a gravitational potential $\phi(\mathbf{w})$ computed as:

$$\phi(\mathbf{w}) = -\frac{2\pi^{1-D/2}\Gamma(D/2)G}{(D-2)l_0^2} \int_{V_D} \frac{d\tilde{m}_{(D)}}{(|\mathbf{x} - \mathbf{x}'|/l_0)^{D-2}} = -\frac{2\pi^{1-D/2}\Gamma(D/2)G}{(D-2)l_0^2} \int_{V_D} \frac{\tilde{\rho}(\mathbf{w}')}{|\mathbf{w} - \mathbf{w}'|^{D-2}} d^D\mathbf{w}'; \quad D \neq 2 \quad (17)$$

$$\phi(\mathbf{w}) = \frac{2G}{l_0^2} \int_{V_2} d\tilde{m}_{(2)} \ln(|\mathbf{x} - \mathbf{x}'|/l_0) = \frac{2G}{l_0^2} \int_{V_2} \tilde{\rho}(\mathbf{w}') \ln|\mathbf{w} - \mathbf{w}'| d^2\mathbf{w}'; \quad D = 2$$

with $\phi(\mathbf{w})$ and $\mathbf{g}(\mathbf{w})$ connected through $\mathbf{g}(\mathbf{w}) = -\nabla_D \phi(\mathbf{w})$, where ∇_D represents the Del (nabla) operator in fractional space.⁷ This general form of the scalar potential can also be derived directly by solving the generalized Laplace/Poisson equations ($\nabla_D^2 \phi(\mathbf{w}) = 0$ and $\nabla_D^2 \phi(\mathbf{w}) = \frac{4\pi G}{l_0^2} \tilde{\rho}(\mathbf{w})$, respectively), as shown in Appendix A at the end of this paper.

There is a fair amount of latitude in the definition of the ∇_D -Del operator and of the other first and second order operators for the case of non-integer dimensional spaces (see [47, 48] for general reviews). The axiomatic bases for spaces with non-integer dimension were introduced by Stillinger [49] and Wilson [44], then refined by Palmer and Stavrinou [50]. Following Eq. (8), a radial Laplacian operator, $\nabla_D^2 f(r) = \frac{1}{r^{D-1}} \frac{d}{dr} \left(r^{D-1} \frac{df}{dr} \right) = \frac{d^2 f}{dr^2} + \frac{(D-1)}{r} \frac{df}{dr}$, for a scalar field f can be derived [49], from which a fractional Laplacian in spherical coordinates follows:

$$\nabla_D^2 f = \frac{1}{r^{D-1}} \frac{\partial}{\partial r} \left(r^{D-1} \frac{\partial f}{\partial r} \right) + \frac{1}{r^2 \sin^{D-2} \theta} \frac{\partial}{\partial \theta} \left(\sin^{D-2} \theta \frac{\partial f}{\partial \theta} \right) + \frac{1}{r^2 \sin^2 \theta \sin^{D-3} \varphi} \frac{\partial}{\partial \varphi} \left(\sin^{D-3} \varphi \frac{\partial f}{\partial \varphi} \right) \quad (18)$$

$$= \left[\frac{\partial^2 f}{\partial r^2} + \frac{(D-1)}{r} \frac{\partial f}{\partial r} \right] + \frac{1}{r^2} \left[\frac{\partial^2 f}{\partial \theta^2} + \frac{(D-2)}{\tan \theta} \frac{\partial f}{\partial \theta} \right] + \frac{1}{r^2 \sin^2 \theta} \left[\frac{\partial^2 f}{\partial \varphi^2} + \frac{(D-3)}{\tan \varphi} \frac{\partial f}{\partial \varphi} \right],$$

which obviously reduces to the standard expression for $D = 3$.

Following Tarasov [47, 48], we will extend the definition for the divergence of a vector field $\mathbf{F} = F_r \hat{\mathbf{r}} + F_\theta \hat{\theta} + F_\varphi \hat{\varphi}$ in spherical coordinates as follows:

⁷ Since ∇_D and all the other operators introduced later in this section will be defined in terms of dimensionless coordinates, the physical dimensions for the gravitational potential ϕ defined in Eq. (17) are the same as those for the gravitational field \mathbf{g} , i.e., both quantities will be measured in m s^{-2} .

$$\begin{aligned}
\operatorname{div}_D \mathbf{F} = \nabla_D \cdot \mathbf{F} &= \left[\frac{1}{r^{D-1}} \frac{\partial}{\partial r} (r^{D-1} F_r) \right] \hat{\mathbf{r}} + \left[\frac{1}{r \sin^{D-2} \theta} \frac{\partial}{\partial \theta} (\sin^{D-2} \theta F_\theta) \right] \hat{\theta} + \left[\frac{1}{r \sin \theta \sin^{D-3} \varphi} \frac{\partial}{\partial \varphi} (\sin^{D-3} \varphi F_\varphi) \right] \hat{\varphi} \\
&= \left[\frac{\partial F_r}{\partial r} + \frac{(D-1)}{r} F_r \right] \hat{\mathbf{r}} + \frac{1}{r} \left[\frac{\partial F_\theta}{\partial \theta} + \frac{(D-2)}{\tan \theta} F_\theta \right] \hat{\theta} + \frac{1}{r \sin \theta} \left[\frac{\partial F_\varphi}{\partial \varphi} + \frac{(D-3)}{\tan \varphi} F_\varphi \right] \hat{\varphi}, \tag{19}
\end{aligned}$$

and assume that the definitions for gradient and curl are not affected by the fractional dimension of the space, thus defining $\operatorname{grad}_D f = \nabla_D f \equiv \nabla f$ and $\operatorname{curl}_D \mathbf{F} = \nabla_D \times \mathbf{u} \equiv \nabla \times \mathbf{u}$.⁸

Adopting the above definitions, it is easy to check that the relation $\nabla_D^2 f = \operatorname{div}_D \operatorname{grad}_D f = \nabla_D \cdot \nabla_D f$ holds without any approximation, and that Eqs. (14) and (17) are connected by $\mathbf{g}(\mathbf{w}) = -\nabla_D \phi(\mathbf{w})$, which actually follows from $\nabla_D \left(\frac{1}{|\mathbf{w}-\mathbf{w}'|^{D-2}} \right) \equiv \nabla \left(\frac{1}{|\mathbf{w}-\mathbf{w}'|^{D-2}} \right) = -(D-2) \frac{\mathbf{w}-\mathbf{w}'}{|\mathbf{w}-\mathbf{w}'|^D}$ (for $D \neq 2$)⁹ with the derivatives taken with respect to \mathbf{w} , while \mathbf{w}' is kept constant.¹⁰ Therefore, the “fractional” gravitational field $\mathbf{g}(\mathbf{w})$ in Eq. (14) can be considered to be “conservative” as it verifies $\nabla_D \times \mathbf{g} = 0$, or $\oint \mathbf{g} \cdot d^\alpha \mathbf{l} = 0$, where $d^\alpha \mathbf{l}$ is an appropriate infinitesimal fractional line element of dimension α ($0 < \alpha \leq 1$). The connection between gravitational field and potential can also be expressed in integral form as $\Delta \Phi = -\int \mathbf{g} \cdot d^\alpha \mathbf{l}$.

If we take the fractional divergence of Eq. (14) and use the fractional relation $\nabla_D \cdot \left(\frac{\mathbf{w}-\mathbf{w}'}{|\mathbf{w}-\mathbf{w}'|^D} \right) = \frac{2\pi^{D/2}}{\Gamma(D/2)} \delta^D(\mathbf{w}-\mathbf{w}')$, we obtain the differential form of the fractional gravitational Gauss’s law:

$$\nabla_D \cdot \mathbf{g}(\mathbf{w}) = -\frac{4\pi G}{l_0^2} \tilde{\rho}(\mathbf{w}). \tag{20}$$

Further integration of this law over a fractional volume V_D of dimension D ($1 < D \leq 3$) and using a fractional version of the divergence theorem, $\oint_{S_d} \mathbf{g}(\mathbf{w}) \cdot d^d \mathbf{a} = \int_{V_D} \nabla_D \cdot \mathbf{g}(\mathbf{w}) d^D \mathbf{w}$, involving a hypersurface S_d of fractional dimension $d = D - 1$ ($0 < d \leq 2$) and infinitesimal surface area $d^d \mathbf{a}$, yields the integral form of the fractional Gauss theorem:

$$\Phi_g^{(D)} = \oint_{S_d} \mathbf{g}(\mathbf{w}) \cdot d^d \mathbf{a} = -\frac{4\pi G}{l_0^2} \int_{V_D} \tilde{\rho}(\mathbf{w}) d^D \mathbf{w} = -\frac{4\pi G}{l_0^2} \tilde{M}_{(D)}. \tag{21}$$

This last equation generalizes our previous Eq. (10), where now $\tilde{M}_{(D)}$ represents the total mass “enclosed” by the hypersurface S_d .¹¹ In cases of high symmetry (spherical, cylindrical, etc.) it can be used to determine the gravitational field \mathbf{g} as it is usually done in standard Newtonian gravity. Combining together the expression for the divergence of the field with the relation between field and potential given above we can also obtain a fractional Poisson equation:

$$\nabla_D^2 \phi(\mathbf{w}) = \frac{4\pi G}{l_0^2} \tilde{\rho}(\mathbf{w}). \tag{22}$$

In Appendix A, we will solve the related fractional Laplace equation $\nabla_D^2 \phi(\mathbf{w}) = 0$, for regions where $\tilde{\rho}(\mathbf{w}) = 0$, and derive the corresponding fractional multipole expansion. Other formulas of Newtonian gravity and potential theory can also be generalized to fractional dimensional cases, but this analysis would go beyond the scope of this paper and will be left to further studies. In the next section, we will apply the ideas developed above to some fundamental models of galactic structures.

⁸ It should be noted that alternative definitions for ∇_D and for the other vector operators exist in the literature. For example [7], from the general definition of the Laplacian $\nabla_D^2 = \left[\frac{\partial^2}{\partial x_1^2} + \frac{\alpha_1-1}{x_1} \frac{\partial}{\partial x_1} \right] + \left[\frac{\partial^2}{\partial x_2^2} + \frac{\alpha_2-1}{x_2} \frac{\partial}{\partial x_2} \right] + \left[\frac{\partial^2}{\partial x_3^2} + \frac{\alpha_3-1}{x_3} \frac{\partial}{\partial x_3} \right]$, with $D = \alpha_1 + \alpha_2 + \alpha_3$ and $0 < \alpha_i \leq 1$, $i = 1, 2, 3$, the Del operator can be defined as: $\nabla_D = \sqrt{\left[\frac{\partial^2}{\partial x_1^2} + \frac{\alpha_1-1}{x_1} \frac{\partial}{\partial x_1} \right]} \hat{\mathbf{x}}_1 + \sqrt{\left[\frac{\partial^2}{\partial x_2^2} + \frac{\alpha_2-1}{x_2} \frac{\partial}{\partial x_2} \right]} \hat{\mathbf{x}}_2 + \sqrt{\left[\frac{\partial^2}{\partial x_3^2} + \frac{\alpha_3-1}{x_3} \frac{\partial}{\partial x_3} \right]} \hat{\mathbf{x}}_3$, where the final approximation is obtained by using a binomial series expansion and neglecting higher-order derivatives and higher powers of the coordinates in the denominators. This approximated formula is valid only in the far-field region (i.e., for $|x_1|, |x_2|, |x_3| \gg 1$), but can be used to define all the other fractional vector operators, such as $\operatorname{grad}_D f \equiv \nabla_D f$, $\operatorname{div}_D \mathbf{F} \equiv \nabla_D \cdot \mathbf{F}$, and $\operatorname{curl}_D \mathbf{F} \equiv \nabla_D \times \mathbf{F}$, for scalar functions $f = f(x_1, x_2, x_3)$ and vector functions $\mathbf{F} = \mathbf{F}(x_1, x_2, x_3)$. With these definitions, the relation $\nabla_D^2 f = \operatorname{div}_D \operatorname{grad}_D f = \nabla_D \cdot \nabla_D f$ is only approximately true.

⁹ For $D = 2$, we have $\nabla_2(\ln |\mathbf{w} - \mathbf{w}'|) \equiv \nabla(\ln |\mathbf{w} - \mathbf{w}'|) = \frac{\mathbf{w} - \mathbf{w}'}{|\mathbf{w} - \mathbf{w}'|^2}$.

¹⁰ The operators defined in Eqs. (18) and (19) as well as the gradient and curl, are now acting on functions of dimensionless spherical coordinates $w = (w_r, w_\theta, w_\varphi) \equiv (r/l_0, \theta, \varphi)$.

¹¹ In Eq. (21), we use dimensionless coordinates \mathbf{w} , so the flux $\Phi_g^{(D)}$ has the same dimensions of the field \mathbf{g} (m s^{-2}). In Eq. (10) we were still using standard coordinates, so the flux $\Phi_g^{(D)}$ was measured in $\text{m}^D \text{s}^{-2}$. The two equations are equivalent also in view of the redefinition of the fractional mass as $m_{(D)} = \tilde{m}_{(D)}/l_0^{3-D}$.

IV. GALACTIC MODELS

From the analysis presented in Sect. III, it is clear that our NFG is intended as a modification of the law of gravity and not of the law of inertia and Newtonian dynamics. However, it is possible that similar modifications might also affect the other forces in nature (e.g., the electromagnetic force, since the theory outlined in Sect. III was originally introduced for the electromagnetic field [7, 33, 34]).¹²

In this way, our interpretation is somewhat in between the two original forms of the MOND theory outlined at the beginning of Sect. II. Nevertheless, we will assume that Newtonian dynamics (i.e., Newton's laws of motion and related consequences, such as conservation principles, etc.) is not affected in any way by our fractional generalizations. A test object, subject to a fractional gravitational field, such as the one described by Eq. (14), will still move in a (classical) 3 + 1 space-time, thus obeying standard laws of dynamics.

The structure and the dynamics of galaxies are described in detail in the seminal monograph by Binney and Tremaine [51]. In the following sub-sections, we will apply our NFG to some fundamental galactic structures and connect our results with the empirical MOND predictions outlined in Sect. II. In this paper, we will limit ourselves to cases of spherical symmetry, leaving other types of symmetries and geometries to future work [52].

A. Spherical symmetry

The gravitational field $\mathbf{g}(w)$, due to a spherically symmetric source mass distribution $\tilde{\rho}(w')$, in a fractal space of dimension $D(w)$ depending on the distance from the center of the coordinate system, can be computed directly by generalizing the standard Newtonian derivation based on the computation of the field due to an infinitesimal spherical shell.

The full derivation is presented in Appendix B. There we show how, starting from Eq. (14), we obtain the following general expression (same as Eq. (B3) in Appendix B):

$$\mathbf{g}_{obs}(w) = -\frac{4\pi G}{l_0^2 w^{D(w)-1}} \int_0^w \tilde{\rho}(w') w'^{D(w)-1} dw' \hat{\mathbf{w}}, \quad (23)$$

which was proved for $1 \leq D \leq 3$.

In the previous equation, we also denoted the gravitational field as the “observed” one, \mathbf{g}_{obs} , as opposed to the “baryonic” \mathbf{g}_{bar} :

$$\mathbf{g}_{bar}(w) = -\frac{4\pi G}{l_0^2 w^2} \int_0^w \tilde{\rho}(w') w'^2 dw' \hat{\mathbf{w}}, \quad (24)$$

for fixed dimension $D = 3$. In other words, we identify the observed and baryonic accelerations g_{obs} and g_{bar} [15] with those obtained in NFG for variable dimension D and for fixed dimension $D = 3$, respectively.

With these NFG assumptions, for spherically symmetric structures, the ratio $(g_{obs}/g_{bar})_{NFG}$ is simply obtained from Eqs. (23) and (24):

$$\left(\frac{g_{obs}}{g_{bar}}\right)_{NFG}(w) = w^{3-D(w)} \frac{\int_0^w \tilde{\rho}(w') w'^{D(w)-1} dw'}{\int_0^w \tilde{\rho}(w') w'^2 dw'}, \quad (25)$$

where the dimension function $D(w)$ needs to be determined either from experimental data or from theoretical considerations. In this section, we will consider the first option, while possible theoretical determination of the dimension function will be left for future work on the subject [52].

In general, to obtain $D(w)$ from experimental data, without fitting any particular set of galactic data, we simply compare the expression in Eq. (25) with the MOND equivalent expression from Eq. (6), $\left(\frac{g_{obs}}{g_{bar}}\right)_{MOND}(w) = \frac{1}{1-e^{-\sqrt{g_{bar}(w)/g_{\dagger}}}}$, or with similar expressions obtained by using the other interpolation functions in Eq. (5). If these

¹² Fractional electrodynamics has already been applied successfully to some fractal media and materials (see again [6, 7] and references therein), thus showing that classical forces can be affected by the dimensionality of space.

two expressions are compatible, we expect to obtain $D(w)$ as a continuous function with values $D \approx 3$ in regions where Newtonian gravity holds. The dimension should then decrease toward $D \approx 2$ in regions where the deep-MOND regime applies, following our general discussion in Sect. II.

B. Point-mass objects

Following Eq. (8), a point-mass m placed at the origin of a D -dimensional space can be represented, in spherical coordinates, by the following mass density:

$$\tilde{\rho}(w') = \frac{m\Gamma(D/2)\delta(w')}{2\pi^{D/2}w'^{D-1}}, \quad (26)$$

which reduces to the standard expression $\tilde{\rho}(w') = \frac{m\delta(w')}{4\pi w'^2}$ for $D = 3$. With this choice for the mass density, assuming $a_0 = Gm/l_0^2$ from Eq. (12), and using the properties of the Dirac delta functions inside the integrals in Eqs. (23)-(25), all the relevant quantities are easily computed.

The y parameter from Eq. (4) simply becomes $y = \frac{g_{bar}}{a_0} = \frac{1}{w^2}$, from which the functions in Eq. (5) corresponding to $(\frac{g_{obs}}{g_{bar}})_{MOND}$ are easily obtained. In particular:

$$\begin{aligned} \nu_n(y) &= \left(\frac{1}{2} + \frac{1}{2}\sqrt{1+4w^{2n}} \right)^{1/n} \\ \hat{\nu}_n(y) &= [1 - \exp(-w^{-n})]^{-1/n} \end{aligned} \quad (27)$$

and

$$\begin{aligned} g_{bar}(w) &= \frac{a_0}{w^2} \\ g_{obs}(w) &= \frac{a_0 2\pi^{1-D(w)/2} \Gamma(D(w)/2)}{w^{D(w)-1}} \\ \left(\frac{g_{obs}}{g_{bar}}\right)_{NFG}(w) &= 2\pi^{1-D(w)/2} \Gamma(D(w)/2) w^{3-D(w)}. \end{aligned} \quad (28)$$

In view of Eq. (6) in Sect. II, the variable dimension $D(w)$ appearing in the second and third lines of the previous equation is obtained by equating the function $(\frac{g_{obs}}{g_{bar}})_{NFG}(w)$ in the same Eq. (28) with either $\nu_n(w)$ or $\hat{\nu}_n(w)$ from Eq. (27), and by solving numerically the resulting equation.

Figure 1 shows all the results for this particular case. The top-left panel illustrates the variable dimension $D(w)$ obtained using the functions in Eq. (27). We can see that the MOND functions are not fully compatible with the NFG analysis at low values for w , where the dimension suddenly changes from $D \approx 3$ in the initial Newtonian regime, to a low value close to zero. This is due to the fact that the equation $(\frac{g_{obs}}{g_{bar}})_{NFG}(w) = \hat{\nu}_1(w)$ (or $\hat{\nu}_2(w)$) admits two possible numerical solutions in this region, where one of the two becomes progressively greater than $D \approx 3$. In the figure we only show values $0 < D \lesssim 3$. At higher values for the variable w , the dimension D progressively decreases toward the $D = 2$ value, as it is to be expected in the deep-MOND regime, following the discussion in Sect. III.

The top-right panel in the figure shows the ratio $\frac{g_{obs}}{g_{bar}}$ computed in two different ways: $(\frac{g_{obs}}{g_{bar}})_{NFG}(w)$ from Eq. (28) with the dimension $D(w)$ obtained before, and $(\frac{g_{obs}}{g_{bar}})_{MOND}(w) = \hat{\nu}_1(w)$ (or $\hat{\nu}_2(w)$), simply using the two MOND functions in Eq. (27). In both cases, the NFG plots (solid lines) match the MOND ones (dotted lines), showing a ratio $\frac{g_{obs}}{g_{bar}} \simeq 1$ at low w within the Newtonian regime. In the deep-MOND high- w range we have instead $\frac{g_{obs}}{g_{bar}} \sim w + \frac{1}{2}$, or $\frac{g_{obs}}{g_{bar}} \sim w$, for the two cases related to $\hat{\nu}_1$ and $\hat{\nu}_2$ respectively, as expected in the MOND model. The results shown in these two top panels of figure 1 are independent of the mass m of the point-like object, and were obtained by using only the $n = 1, 2$ values for the general MOND function $\hat{\nu}_n$ in Eq. (5). Using $n > 2$ values for the same function $\hat{\nu}_n$ does not yield results which are much different from the $n = 2$ ones.¹³

¹³ Using MOND functions ν_n , instead of $\hat{\nu}_n$, yields very similar results for all values of n . Therefore, we have considered only the $\hat{\nu}_n$ family of MOND interpolation functions in this work.

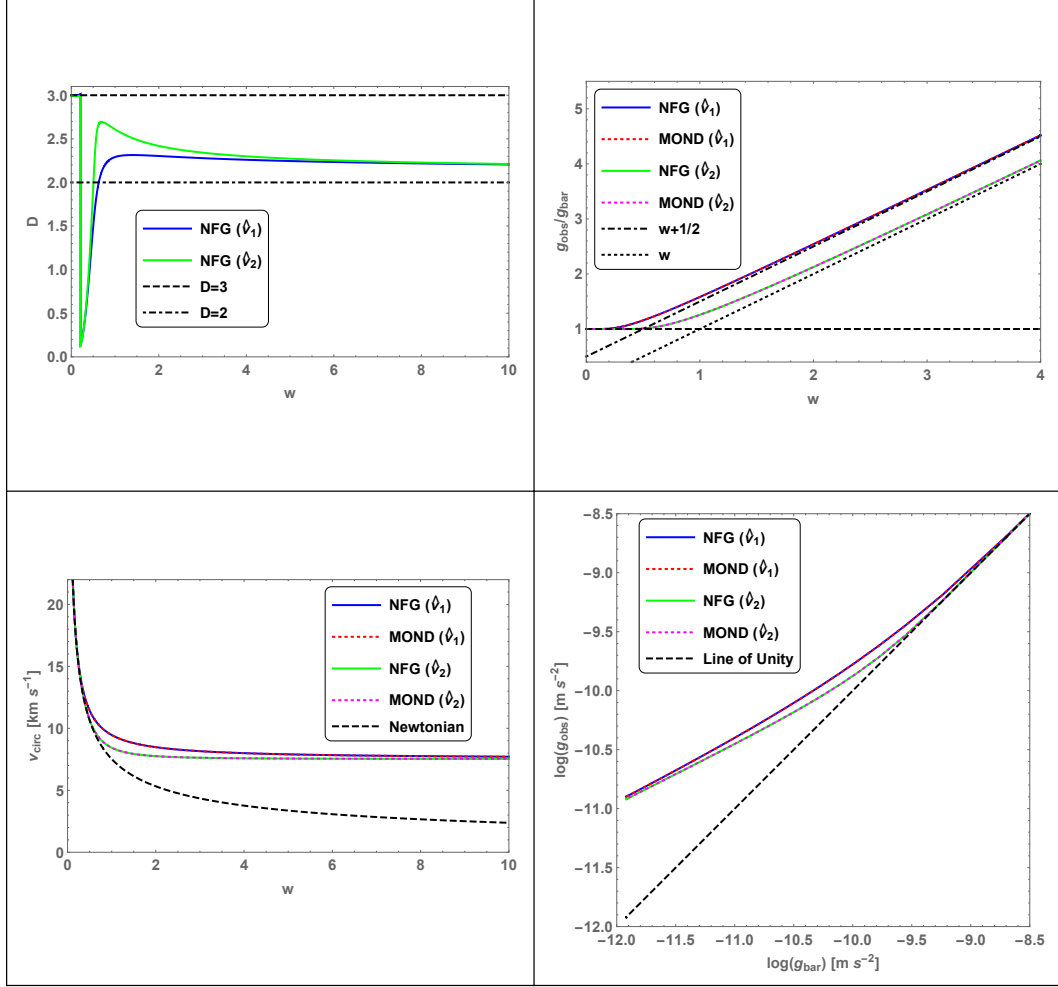


FIG. 1. Point-mass object results. Top-left panel: NFG variable dimension D (w) for MOND interpolation functions $\hat{\nu}_1$ and $\hat{\nu}_2$. Other panels: comparison of NFG results (solid lines) with equivalent MOND predictions (dotted lines) for the two different interpolation functions. Also shown: Newtonian behavior-Line of Unity (black-dashed lines).

The bottom-left panel shows circular velocity plots corresponding to the previously analyzed cases, and compared with the purely Newtonian case. For this panel, as well as for the bottom-right one, we have assumed a mass $m \approx 2 \times 10^5 M_\odot \approx 4 \times 10^{35} \text{ kg}$, typical of globular clusters in our Galaxy [51], but the results would be similar for any other choice of mass m . In this panel the NFG circular speeds are computed as $v_{circ} = \sqrt{g_{obs}(w) w l_0} / 10^3 [\text{km s}^{-1}]$ with $l_0 \approx \sqrt{\frac{Gm}{a_0}} \simeq 4.72 \times 10^{17} \text{ m}$. The MOND circular speeds are computed as $v_{circ} = \sqrt{g_{bar}(w) \hat{\nu}_1(w) w l_0} / 10^3 [\text{km s}^{-1}]$ (or using $\hat{\nu}_2$ instead of $\hat{\nu}_1$) and the purely Newtonian speed is $v_{circ} = \sqrt{g_{bar}(w) w l_0} / 10^3 [\text{km s}^{-1}]$. As seen from the panel, there is perfect agreement between the respective ($\hat{\nu}_1$ or $\hat{\nu}_2$) NFG and MOND cases, showing the expected flattening of the circular speed plots at high- w , as opposed to the standard Newtonian decrease of circular speed with radial distance ($w_{circ} \sim 1/\sqrt{w}$ for Newtonian behavior).

Finally, the bottom right panel is similar to the $\log(g_{obs})$ vs. $\log(g_{bar})$ plots widely used in the literature (see Fig. 3 in Ref. [15] or the figures in Ref. [16]) to illustrate the validity of the general MOND-RAR relation in Eq. (6). Compared to the *Line of Unity*, representing the purely Newtonian case, there is again perfect agreement over several orders of magnitude between plots obtained with our NFG model, using $g_{obs}(w)$ and $g_{bar}(w)$ from Eq. (28), and MOND plots where $g_{obs}(w) = \hat{\nu}_1(w) g_{bar}(w)$ (or $g_{obs}(w) = \hat{\nu}_2(w) g_{bar}(w)$).

Apart from the discontinuity at low- w in the top-left panel, which will disappear in the next two cases analyzed in this section, the study of the point-mass case already shows that the variable-dimension effect of NFG can be equivalent to the MOND-RAR model. In the next two sub-sections we will confirm this result using two other

spherically symmetric cases.

C. Homogeneous sphere

A homogeneous sphere of radius R and total mass M will have constant mass density $\rho = \frac{3M}{4\pi R^3}$ inside the sphere and $\rho = 0$ outside. Rescaling all distances as usual, $w' = r/l_0$, $W = R/l_0$, and using a Heaviside step function H we can write the rescaled mass density as:

$$\tilde{\rho}(w') = \frac{3M}{4\pi W^3} H(W - w'). \quad (29)$$

We then follow the same procedure outlined in the previous subsection IV B. The y parameter is easily computed as:

$$y = \frac{g_{bar}}{a_0} = \frac{1}{W^3 w^2} [W^3 + (w^3 - W^3) H(W - w)], \quad (30)$$

from which the MOND functions $\hat{\nu}_1$ and $\hat{\nu}_2$ also follow. Functions $g_{obs}(w)$, $g_{bar}(w)$, and their ratio $(\frac{g_{obs}}{g_{bar}})_{NFG}(w)$ will follow from Eqs. (23)-(25), with the dimension $D(w)$ obtained by solving numerically the equation $(\frac{g_{obs}}{g_{bar}})_{NFG}(w) = \hat{\nu}_1(w)$ (or $\hat{\nu}_2(w)$). The total mass is chosen to be the same as the one used in the point-mass case, i.e., $M \approx 2 \times 10^5 M_\odot \approx 4 \times 10^{35} \text{ kg}$, typical of globular clusters. The other physical parameter $W = R/l_0$ is chosen as $W = 0.1$. We will use the same value in the next sub-section for the Plummer model (see Sect. IV D) and this choice will be justified in terms of the astrophysical parameters of globular clusters.

Figure 2 shows the results for this case, in the same way of figure 1 previously. The top left panel illustrates the dimension functions $D(w)$ for the two cases being considered. This time, the dimension functions are uniquely defined and continuous over the whole range: at low- w values, $D \approx 3$ in the Newtonian regime, then the dimension continuously decreases approaching the value $D \approx 2$ in the deep-MOND regime, as expected.

The top-right panel shows the same two regimes, Newtonian and deep-MOND, in terms of the $\frac{g_{obs}}{g_{bar}}$ ratio: close to unity at low- w (Newtonian) and approaching asymptotically $w + 1/2$ (or w) at high- w (deep-MOND). Finally, the two bottom panels show the equivalent circular speed and log-log plots, with perfect correspondence between the NFG and MOND computations (obtained with the same procedure outlined above for figure 1).

D. Plummer model

The last spherical model considered in this section is based on the Plummer gravitational potential $\phi(r) = -\frac{GM}{\sqrt{r^2 + b^2}}$ and related mass density $\rho(r) = \frac{3M}{4\pi b^3} \left(1 + \frac{r^2}{b^2}\right)^{-5/2}$, where M is the total mass of the system and b is the Plummer scale length [51]. As we did for the homogeneous model in the previous sub-section, we rescale all distances, $w' = r/l_0$, $W = b/l_0$, and obtain the effective mass density:

$$\tilde{\rho}(w') = \frac{3M}{4\pi W^3} \left(1 + \frac{w'^2}{W^2}\right)^{-5/2}. \quad (31)$$

Always assuming $a_0 = \frac{GM}{l_0^2}$ and using Eq. (24), we compute $y = \frac{g_{bar}}{a_0} = \frac{w}{W^3} \left(1 + \frac{w^2}{W^2}\right)^{-3/2}$ and then all other quantities follow from the general equations (23)-(25) as in the previous cases, with the integrations performed either analytically or numerically. The Plummer model is usually associated with spherical structures such as globular clusters, therefore we use again the reference mass $M \approx 2 \times 10^5 M_\odot \approx 4 \times 10^{35} \text{ kg}$, which yields $l_0 = \sqrt{\frac{GM}{a_0}} \simeq 4.72 \times 10^{17} \text{ m}$. Since the typical half-mass radius of globular clusters in our Galaxy is $r_h \approx 3 \text{ pc} \approx 10^{17} \text{ m}$ [51], and for the Plummer mass density above $r_h/b \simeq 1.30$, we estimate $b \simeq 7.10 \times 10^{16} \text{ m}$ and thus $W = b/l_0 \approx 0.1$, as also used in sub-section IV C.

Figure 3, modeled after the first two figures, summarizes all results for this case. Once again, the top-left panel shows dimension functions $D(w)$ consistent with our NFG model based on fractional gravity: the effective dimension

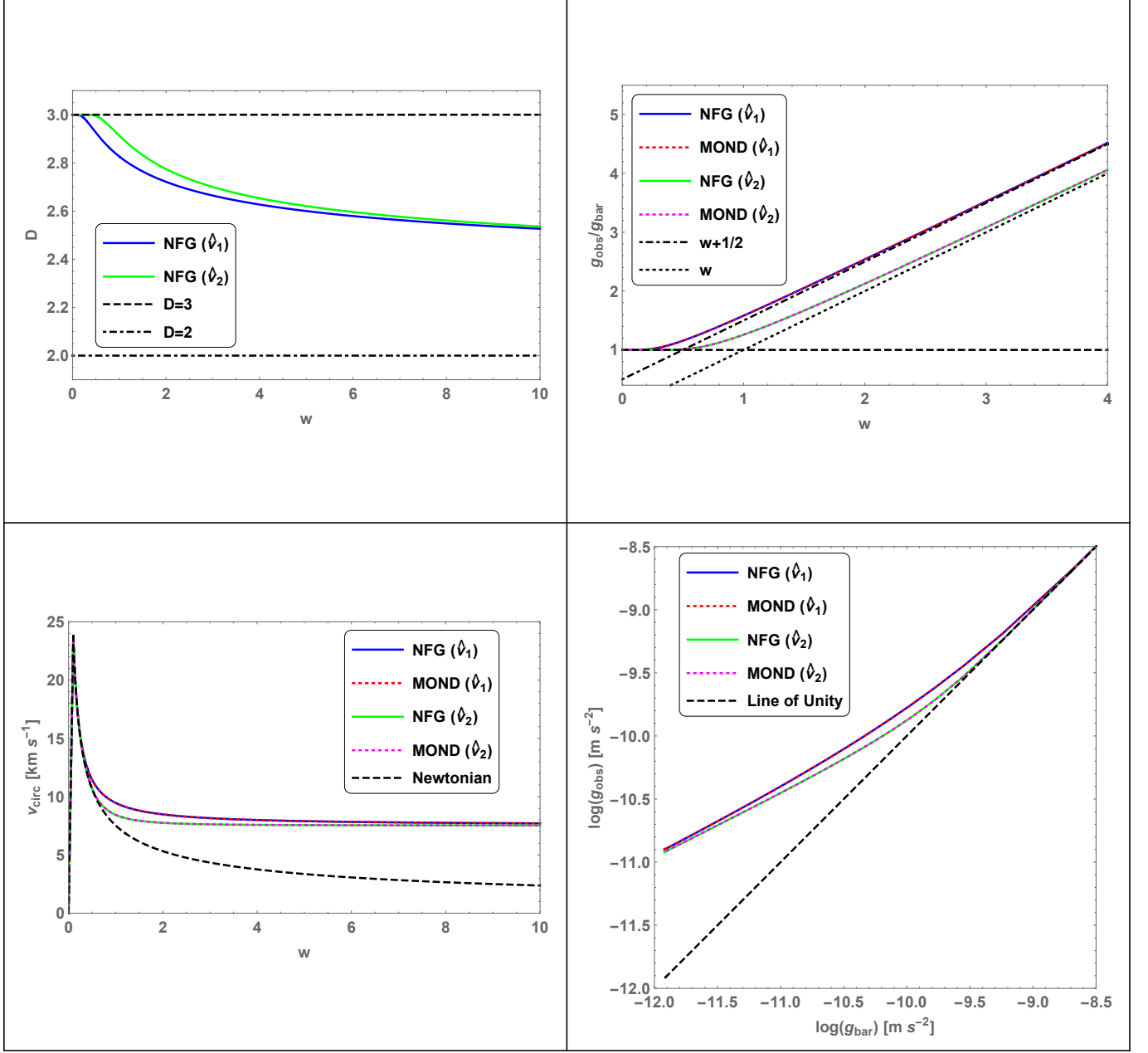


FIG. 2. Homogeneous sphere results. Top-left panel: NFG variable dimension $D(w)$ for MOND interpolation functions $\hat{\nu}_1$ and $\hat{\nu}_2$. Other panels: comparison of NFG results (solid lines) with equivalent MOND predictions (dotted lines) for the two different interpolation functions. Also shown: Newtonian behavior-Line of Unity (black-dashed lines).

of the physical space decreases from the standard Newtonian $D \approx 3$ value toward the deep-MOND $D \approx 2$ value asymptotically.¹⁴ This is also reflected in the top-right panel, by using the $\frac{g_{\text{obs}}}{g_{\text{bar}}}$ ratios instead. The two bottom panels in figure 3, also confirm that our NFG model can yield the same results of the standard MOND theory, but with circular speed plots and log-log plots now explained by our variable-dimension effect, as opposed to just an empirical MOND-RAR relation.

¹⁴ In all these figures, we limited the range of w between 0 and 10. Plotting the top-left panels for $w \gg 10$ would show that, in fact, $D \rightarrow 2$ for large values of w .

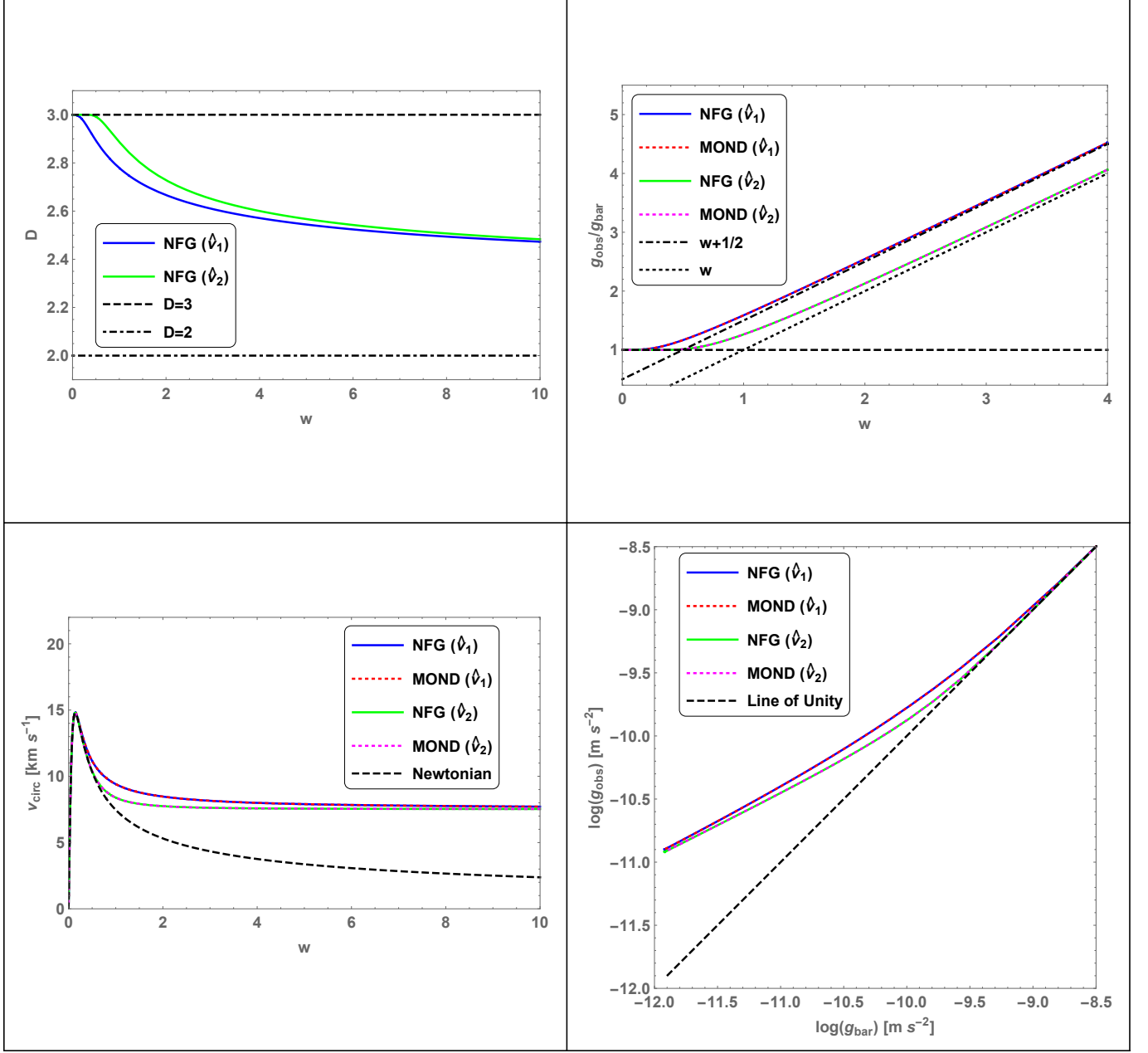


FIG. 3. Plummer model results. Top-left panel: NFG variable dimension D (w) for MOND interpolation functions $\hat{\nu}_1$ and $\hat{\nu}_2$. Other panels: comparison of NFG results (solid lines) with equivalent MOND predictions (dotted lines) for the two different interpolation functions. Also shown: Newtonian behavior-Line of Unity (black-dashed lines).

Although in this section we used globular clusters and their astrophysical data in our models, the NFG analysis can be easily extended to any other spherical stellar structure, such as dwarf spheroidal galaxies or others. Additional simulations corresponding to other choices of spherical stellar structures, with different mass densities and different astrophysical data, produced results similar to those in Figs. 1-3 and, therefore, will not be included in the current work.

V. CONCLUSION

In this work, we outlined a possible explanation of the MOND theory and related RAR in terms of a novel fractional gravity model. We considered the possibility that Newtonian gravity might act on a metric space of variable dimension $D \leq 3$, when applied to galactic scales, and developed the mathematical basis of a classical NFG.

In particular, the MOND acceleration scale a_0 , or the equivalent RAR acceleration parameter $g_{\dagger} = 1.20 \times 10^{-10} \text{ m s}^{-2}$, can be related to a length scale $l_0 \approx \sqrt{\frac{GM}{a_0}}$ which is naturally required for dimensional reasons when applying fractional calculus to physics.

We have shown that, at least for some fundamental spherically-symmetric cases, our NFG can reproduce the same results of the MOND-RAR models, and that the deep-MOND regime can be achieved by continuously decreasing the space dimension D toward a limiting value of $D \approx 2$.

Future work on the subject [52] will be needed to test the NFG hypothesis. This model will need to be extended to galactic structures with axial symmetry and detailed fitting to galactic rotation curves will also need to be performed, before NFG can be considered a viable alternative model. Lastly, the origin of the supposed continuous variation of the space dimension D has to be determined, possibly arising from a relativistic version of fractional gravity.

ACKNOWLEDGMENTS

This work was supported by a Faculty Fellowship awarded by the Frank R. Seaver College of Science and Engineering, Loyola Marymount University. The author also wishes to acknowledge useful suggestions by Dr. Ben Fitzpatrick regarding numerical computations with Mathematica.

Appendix A: Fractional Laplace equation and the multipole expansion

In this section we will consider the fractional version of the Laplace equation, in order to confirm our fundamental Eq. (17) in Sect. III. Limited studies of fractional gravity exist in the literature [53, 54] but, to our knowledge, they do not fully discuss a possible NFG as outlined in this paper.¹⁵

The Laplace equation in spherical coordinates for a D -dimensional space follows from the Laplacian operator in Eq. (18):¹⁶

$$\nabla_D^2 \phi = \frac{1}{r^{D-1}} \frac{\partial}{\partial r} \left(r^{D-1} \frac{\partial \phi}{\partial r} \right) + \frac{1}{r^2 \sin^{D-2} \theta} \frac{\partial}{\partial \theta} \left(\sin^{D-2} \theta \frac{\partial \phi}{\partial \theta} \right) + \frac{1}{r^2 \sin^2 \theta \sin^{D-3} \varphi} \frac{\partial}{\partial \varphi} \left(\sin^{D-3} \varphi \frac{\partial \phi}{\partial \varphi} \right) = 0, \quad (\text{A1})$$

where the gravitational potential ϕ can be a function of the standard “physical” coordinates (r, θ, φ) or of the equivalent dimensionless coordinates $(w_r = r/l_0, w_\theta = \theta, w_\varphi = \varphi)$. In this section, we will simply leave all equations in standard spherical coordinates and we will omit the scale length l_0 in most equations.

Eq. (A1) is separable [49, 50], i.e., $\phi(r, \theta, \varphi) = R(r)\Theta(\theta)\Phi(\varphi)$ and the resulting radial and angular equations are:

$$\begin{aligned} \left[\frac{1}{r^{D-1}} \frac{d}{dr} \left(r^{D-1} \frac{d}{dr} \right) + \frac{k_1}{r^2} \right] R(r) &= 0 \\ \left[\frac{1}{\sin^{D-2} \theta} \frac{d}{d\theta} \left(\sin^{D-2} \theta \frac{d}{d\theta} \right) - k_1 - \frac{k_2}{\sin^2 \theta} \right] \Theta(\theta) &= 0 \\ \left[\frac{1}{\sin^{D-3} \varphi} \frac{d}{d\varphi} \left(\sin^{D-3} \varphi \frac{d}{d\varphi} \right) + k_2 \right] \Phi(\varphi) &= 0 \end{aligned} \quad (\text{A2})$$

where the separation constants take the values $k_2 = m(m+D-3)$, $m = 0, 1, 2, \dots$ and $k_1 = -l(l+D-2)$, $l = 0, 1, 2, \dots$ with $m \leq l$.

The complete solution to the angular equations can be found in Appendix B of Ref. [50], where both angular functions Θ and Φ can be expressed in terms of Gegenbauer polynomials [56–58]. Here, we will limit our analysis to

¹⁵ Recently, a connection between MOND and fractional theories was proposed by Giusti [55], while our work was being finalized. In this approach, Giusti used a different gravitational potential, compared to our Eq. (17), and a scale length $l = \frac{2}{\pi} \sqrt{\frac{GM}{a_0}}$ to establish a connection with the MOND theory.

¹⁶ This equation assumes a constant value for the dimension D , although not necessarily an integer one. The theory of NFG outlined in Sect. III considered a variable dimension D as a function of the field point coordinates. If we assume that D varies slowly with these coordinates, then the results obtained in this section will be approximately true and valid also in the case of a variable dimension.

cases of axial symmetry, i.e., $\phi(r, \theta) = R(r)\Theta(\theta)$ corresponding to $k_2 = m = 0$ ($\Phi(\varphi) = 1$). In this case, the radial equation admits two independent solutions $R(r) = r^l$ and $R(r) = 1/r^{l+D-2}$, while the angular solution is given in terms of Gegenbauer polynomials in $\cos \theta$: $\Theta(\theta) = C_l^{(\frac{D}{2}-1)}(\cos \theta)$.

Gegenbauer polynomials (a.k.a., ultraspherical functions) $C_l^{(\lambda)}(x)$ [56] form a set of orthogonal polynomials defined over the interval $(-1, 1)$ and with constraints $\lambda > -\frac{1}{2}, \lambda \neq 0$. The weight function is $w(x) = (1 - x^2)^{\lambda - \frac{1}{2}}$, i.e., the orthogonality condition is $\int_{-1}^{+1} w(x)C_l^{(\lambda)}(x)C_{l'}^{(\lambda)}(x)dx = 0$ for $l \neq l'$ and the normalization factor is $h_l = \frac{2^{1-2\lambda}\pi\Gamma(l+2\lambda)}{(l+\lambda)(\Gamma(\lambda))^2 l!}$, that is, $\int_{-1}^{+1} (C_l^{(\lambda)}(x))^2 w(x)dx = h_l$. The Rodriguez formula for the Gegenbauer polynomials is $C_l^{(\lambda)}(x) = \frac{1}{\kappa_l w(x)} \frac{d^l}{dx^l} (w(x)(F(x))^l)$ with $F(x) = 1 - x^2$ and $\kappa_l = \frac{(-2)^l(\lambda + \frac{1}{2})_l l!}{(2\lambda)_l}$,¹⁷ and the main generating function is: $(1 - 2xz + z^2)^{-\lambda} = \sum_{l=0}^{\infty} C_l^{(\lambda)}(x)z^l$ for $|z| < 1$.

Adapting these definitions and properties to the case of our physical solutions above, we set $x \equiv \cos \theta$ and $\lambda \equiv \frac{D}{2} - 1$. The constraints for λ limit the use of Gegenbauer polynomials to the case $D > 1$, $D \neq 2$ and the overall ortho-normality condition can be written as:

$$\int_0^{\pi} C_l^{(\frac{D}{2}-1)}(\cos \theta) C_{l'}^{(\frac{D}{2}-1)}(\cos \theta) \sin^{D-2} \theta d\theta = h_l \delta_{ll'} \quad (\text{A3})$$

$$h_l = \frac{2^{3-D}\pi\Gamma(l+D-2)}{(l+\frac{D}{2}-1) [\Gamma(\frac{D}{2}-1)]^2 l!}.$$

The first few Gegenbauer polynomials in $\cos \theta$ are:

$$C_0^{(\frac{D}{2}-1)}(\cos \theta) = 1; \quad C_1^{(\frac{D}{2}-1)}(\cos \theta) = (D-2) \cos \theta; \quad C_2^{(\frac{D}{2}-1)}(\cos \theta) = \left(\frac{D}{2}-1\right) (D \cos^2 \theta - 1); \dots \quad (\text{A4})$$

It is evident that, in the case $D = 3$, the Gegenbauer polynomials will reduce to standard Legendre polynomials $P_l(\cos \theta)$. In the case of possible dependence of the gravitational potential on both angular variables θ and φ [50], the ultraspherical functions will reduce instead to standard spherical harmonics $Y_{l,m}(\theta, \varphi)$, for $D = 3$. Considering just the case of axial symmetry, the general solution for a given boundary condition $\phi(R, \theta) = \phi_0(\theta)$ is:

$$\phi(r, \theta) = \sum_{l=0}^{\infty} \left(A_l r^l + \frac{B_l}{r^{l+D-2}} \right) C_l^{(\frac{D}{2}-1)}(\cos \theta) \quad (\text{A5})$$

$$A_l = \frac{1}{R^l h_l} \int_0^{\pi} \phi_0(\theta) C_l^{(\frac{D}{2}-1)}(\cos \theta) \sin^{D-2} \theta d\theta$$

$$B_l = \frac{R^{l+D-2}}{h_l} \int_0^{\pi} \phi_0(\theta) C_l^{(\frac{D}{2}-1)}(\cos \theta) \sin^{D-2} \theta d\theta,$$

where the coefficients A_l and B_l were obtained by using Eq. (A3).

For a single point-mass placed at the origin, $\tilde{\rho}(\mathbf{r}) = \tilde{m}_{(D)}\delta^{(D)}(\mathbf{r})$, the potential following the first line of Eq. (A5) must consist only of the $l = 0$ term, due to spherical symmetry. Requiring also the potential to be zero at infinity implies $\phi(r) = \frac{B_0}{r^{D-2}}$, from which $\nabla_D^2 \phi = -\frac{B_0(D-2)2\pi^{D/2}\delta^{(D)}(\mathbf{r})}{\Gamma(D/2)}$, following $\nabla_D \cdot (\frac{\hat{\mathbf{r}}}{r^{D-1}}) = \frac{2\pi^{D/2}}{\Gamma(D/2)}\delta^{(D)}(\mathbf{r})$ and $\nabla_D \cdot (\frac{1}{r^{D-2}}) = -(D-2)\frac{\hat{\mathbf{r}}}{r^{D-1}}$. On the other hand, the generalized Poisson equation (22) implies $\nabla_D^2 \phi = 4\pi G \tilde{m}_{(D)}\delta^{(D)}(\mathbf{r})$ and combining both results we obtain the coefficient $B_0 = -\frac{2\pi^{1-D/2}\Gamma(D/2)G\tilde{m}_{(D)}}{(D-2)}$ and the potential of a point-mass becomes $\phi(r) = -\frac{2\pi^{1-D/2}\Gamma(D/2)G\tilde{m}_{(D)}}{(D-2)r^{D-2}}$, thus confirming the first line of Eq. (17).

Since the fractal gradient we introduced in Sect. III is the same as the standard one, the gravitational field we obtain from the point mass potential above, confirms also our previous Eq. (11) in Sect. III which was originally

¹⁷ The Pochhammer's symbol $(a)_l$ is defined as $(a)_0 = 1$, $(a)_l = a(a+1)(a+2)\dots(a+l-1) = \Gamma(a+l)/\Gamma(a)$.

introduced in a heuristic way. In fact, adding the appropriate scale length l_0 into the equations for dimensional correctness, we obtain $\mathbf{g} = -\nabla_D \phi = -\frac{2\pi^{1-D/2}\Gamma(D/2)G\tilde{m}_{(D)}}{l_0^2} \frac{(\mathbf{r}/l_0)}{(r/l_0)^{D-1}}$, which is equivalent to Eq. (11).

By using the generating function of the Gegenbauer polynomials above, rewritten with $x = \cos \theta'$, $\lambda = \frac{D}{2} - 1$, and $z = r'/r$ or $z = r/r'$, for $r' < r$ and $r < r'$ respectively, we can write:

$$\frac{1}{|\mathbf{r} - \mathbf{r}'|^{D-2}} = \begin{cases} \frac{1}{r^{D-2}} \sum_{l=0}^{\infty} \left(\frac{r'}{r}\right)^l C_l^{\left(\frac{D}{2}-1\right)}(\cos \theta') ; \text{ for } r' < r \\ \frac{1}{r'^{D-2}} \sum_{l=0}^{\infty} \left(\frac{r}{r'}\right)^l C_l^{\left(\frac{D}{2}-1\right)}(\cos \theta') ; \text{ for } r < r' \end{cases} . \quad (\text{A6})$$

Using the first line of the last equation combined with Eq. (17), we can derive a generalized multipole expansion for a localized charge distribution $\rho = \rho(r', \theta')$ in the case $r \gg r'$:

$$\phi(\mathbf{r}) = -\frac{2\pi^{1-D/2}\Gamma(D/2)G}{(D-2)} \int_{V_D} \frac{\tilde{\rho}(\mathbf{r}') dV_D}{|r - r'|^{D-2}} = -\frac{2\pi^{1-D/2}\Gamma(D/2)G}{(D-2)} \sum_{l=0}^{\infty} \frac{1}{r^{D-2+l}} \int_{V_D} \tilde{\rho}(\mathbf{r}') (r')^l C_l^{\left(\frac{D}{2}-1\right)}(\cos \theta') dV_D, \quad (\text{A7})$$

with the first two terms representing the monopole and dipole moments:

$$\begin{aligned} \phi_{mon}(\mathbf{r}) &= -\frac{2\pi^{1-D/2}\Gamma(D/2)G}{(D-2)r^{D-2}} \int_{V_D} \tilde{\rho}(\mathbf{r}') dV_D = -\frac{2\pi^{1-D/2}\Gamma(D/2)G\tilde{M}_{(D)}}{(D-2)r^{D-2}} \\ \phi_{dip}(\mathbf{r}) &= -\frac{2\pi^{1-D/2}\Gamma(D/2)G}{(D-2)r^{D-1}} \int_{V_D} \tilde{\rho}(\mathbf{r}') r' (D-2) \cos \theta' dV_D = -\frac{2\pi^{1-D/2}\Gamma(D/2)G\tilde{\mathbf{p}}_{(D)} \cdot \hat{\mathbf{r}}}{r^{D-1}}, \end{aligned} \quad (\text{A8})$$

where $\tilde{M}_{(D)}$ is the total D-dimensional mass and $\tilde{\mathbf{p}}_{(D)} = \int_{V_D} \mathbf{r}' \rho(\mathbf{r}') dV_D$ is the D-dimensional dipole moment.

Again, using the standard gradient operator it is easy to obtain the corresponding monopole and dipole terms for the gravitational field:

$$\begin{aligned} \mathbf{g}_{mon}(\mathbf{r}) &= -\frac{2\pi^{1-D/2}\Gamma(D/2)G\tilde{M}_{(D)}}{r^{D-1}} \hat{\mathbf{r}} \\ \mathbf{g}_{dip}(\mathbf{r}) &= -\frac{2\pi^{1-D/2}\Gamma(D/2)G\tilde{\mathbf{p}}_{(D)}}{r^D} [(D-1) \cos \theta \hat{\mathbf{r}} + \sin \theta \hat{\theta}], \end{aligned} \quad (\text{A9})$$

with the monopole term consistent with our previous analysis and with Eq. (11) in Sect. III.

We can also consider the potential of a thin shell of radius a and surface mass density $\sigma(\theta)$ at fixed radius $r = a$. In this case “interior” ($r \leq a$) and “exterior” ($r \geq a$) solutions can be written as:

$$\begin{aligned} \phi_{int}(r, \theta) &= \sum_{l=0}^{\infty} A_l r^l C_l^{\left(\frac{D}{2}-1\right)}(\cos \theta) \\ \phi_{ext}(r, \theta) &= \sum_{l=0}^{\infty} \frac{B_l}{r^{l+D-2}} C_l^{\left(\frac{D}{2}-1\right)}(\cos \theta) \end{aligned} \quad (\text{A10})$$

since the potential at the center must be non singular and the potential at infinity is assumed to be zero. Continuity at $r = a$ and orthogonality of the C_l functions also implies $B_l = A_l a^{2l+D-2}$.

Following a procedure similar to the one outlined in Sect. 2.4 of Ref. [51] for the standard $D = 3$ case, we can expand the surface mass density of the thin shell as $\sigma(\theta) = \sum_{l=0}^{\infty} \sigma_l C_l^{\left(\frac{D}{2}-1\right)}(\cos \theta)$ and, using the ortho-normality of the C_l functions, also obtain:

$$\sigma_l = \frac{1}{h_l} \int_0^\pi \sigma(\theta) C_l^{\left(\frac{D}{2}-1\right)}(\cos \theta) \sin^{D-2} \theta d\theta. \quad (\text{A11})$$

Gauss's theorem (20) applied to a small piece of the shell yields $[\frac{\partial \phi_{ext}}{\partial r}]_{r=a} - [\frac{\partial \phi_{int}}{\partial r}]_{r=a} = 4\pi G\sigma(\theta)$ so that combining this equation with Eq. (A10) and the $\sigma(\theta)$ expansion above, another relation between the A_l and the B_l coefficients can be derived: $-\sum_{l=0}^{\infty} [(l+D-2)B_l a^{-(l+D-1)} + lA_l a^{l-1}] C_l^{(\frac{D}{2}-1)}(\cos\theta) = 4\pi G \sum_{l=0}^{\infty} \sigma_l C_l^{(\frac{D}{2}-1)}(\cos\theta)$. Using this relation and the previous one between these coefficients, it is then possible to extract them explicitly:

$$\begin{aligned} A_l &= -\frac{4\pi G a^{-(l-1)}}{2l+D-2} \sigma_l \\ B_l &= -\frac{4\pi G a^{l+D-1}}{2l+D-2} \sigma_l \end{aligned} \quad (A12)$$

The interior and exterior potentials are then obtained:

$$\begin{aligned} \phi_{int}(r, \theta) &= -4\pi G a \sum_{l=0}^{\infty} \left(\frac{r}{a}\right)^l \frac{\sigma_l}{2l+D-2} C_l^{(\frac{D}{2}-1)}(\cos\theta) \\ \phi_{ext}(r, \theta) &= -4\pi G a \sum_{l=0}^{\infty} \left(\frac{a}{r}\right)^{l+D-2} \frac{\sigma_l}{2l+D-2} C_l^{(\frac{D}{2}-1)}(\cos\theta) \end{aligned} \quad (A13)$$

with σ_l given by Eq. (A11). Finally, the potential of a solid body is evaluated by breaking it into a series of concentric shells. Let $\delta\sigma_l(a)$ be the σ -coefficient of the shell lying between a and $a+\delta a$, and $\delta\phi(r, \theta; a)$ the corresponding potential at r . Following Eq. (A11) with $\sigma(\theta) = \rho(a, \theta) \delta a$ we can write $\delta\sigma_l(a) = \left[\frac{1}{h_l} \int_0^\pi d\theta \sin^{D-2} \theta C_l^{(\frac{D}{2}-1)}(\cos\theta) \rho(a, \theta) \right] \delta a \equiv \rho_l(a) \delta a$. Substituting these values of $\delta\sigma_l$ into Eq. (A13) and summing all contributions over all possible values for a we obtain the potential at r generated by the entire collection of shells:

$$\begin{aligned} \phi(r, \theta) &= \sum_{a=0}^r \delta\phi_{ext} + \sum_{a=r}^{\infty} \delta\phi_{int} \\ &= -4\pi G \sum_{l=0}^{\infty} \frac{C_l^{(\frac{D}{2}-1)}(\cos\theta)}{2l+D-2} \left[\frac{1}{r^{(l+D-2)}} \int_0^r da a^{l+D-1} \rho_l(a) + r^l \int_r^{\infty} \frac{da}{a^{l-1}} \rho_l(a) \right] \\ \rho_l(a) &= \frac{1}{h_l} \int_0^\pi d\theta \sin^{D-2} \theta C_l^{(\frac{D}{2}-1)}(\cos\theta) \rho(a, \theta), \end{aligned} \quad (A14)$$

with h_l given by Eq. (A3).

Eq. (A14) represents the multipole expansion for the gravitational potential ϕ in the case of an axially symmetric distribution of matter, for a generalized dimension $D > 1$ ($D \neq 2$). A more general expansion formula can be derived for the case $\phi(r, \theta, \varphi)$ by using two sets of ultraspherical functions, but this goes beyond the scope of the current work. It is easy to check that the multipole expansion above for the simple case of a point mass at the origin, i.e., $\tilde{\rho}(a) = \tilde{m}_{(D)} \delta^{(D)}(\mathbf{a}) = \tilde{m}_{(D)} \frac{\Gamma(D/2)}{2\pi^{D/2} a^{D-1}} \delta(a)$, would be limited to the $l = 0$ terms and yield $\phi(r, \theta) = -4\pi G \frac{1}{D-2} \left[\frac{1}{r^{D-2}} \int_0^r da a^{D-1} \tilde{m}_{(D)} \frac{\Gamma(D/2)}{2\pi^{D/2} a^{D-1}} \delta(a) \right] = -\frac{2\pi^{1-D/2} \Gamma(D/2) G \tilde{m}_{(D)}}{(D-2)r^{D-2}}$, which again confirms our previous equation (17), for $D \neq 2$.

The special case $D = 2$ corresponds to the classic Dirichlet problem for a circle and the Poisson kernel (see for example Ref. [59]). In fact, adapting Eqs. (A1) and (A2) to the case $D = 2$ and considering a separable solution of the type $\phi(r, \theta) = R(r)\Theta(\theta)$, as was done for the general $D \neq 2$ case above, we obtain:

$$\begin{aligned} \nabla_{(2)}^2 \phi &= \frac{1}{r} \frac{\partial}{\partial r} \left(r \frac{\partial \phi}{\partial r} \right) + \frac{1}{r^2} \frac{\partial^2 \phi}{\partial \theta^2} = 0 \\ \left[\frac{1}{r} \frac{d}{dr} \left(r \frac{d}{dr} \right) - \frac{l^2}{r^2} \right] R(r) &= 0 \\ \left[\frac{d^2}{d\theta^2} + l^2 \right] \Theta(\theta) &= 0, \end{aligned} \quad (A15)$$

where θ can now be considered the polar angle and $l = 0, 1, 2, \dots$ as before. Solutions to the radial and angular equations are:

$$\begin{aligned}\phi_0(r, \theta) &= (A_0 + B_0\theta) (C_0 \ln r + D_0) \\ \phi_l(r, \theta) &= [A_l \cos(l\theta) + B_l \sin(l\theta)] (C_l r^l + D_l r^{-l}); \quad l \neq 0\end{aligned}\tag{A16}$$

Setting $B_0 = 0$, due to the periodicity of the solution, renaming the constants $A_0 D_0 \rightarrow \frac{a_0}{2}, \frac{a'_0}{2}$, $A_0 C_0 \rightarrow \frac{c_0}{2}$, $A_l C_l \rightarrow a_l$, $B_l C_l \rightarrow b_l$, $A_l D_l \rightarrow c_l$, and $B_l D_l \rightarrow d_l$, we can write the interior and exterior solutions to a circle of radius R as:¹⁸

$$\begin{aligned}\phi_{int}(r, \theta) &= \frac{a_0}{2} + \sum_{l=1}^{\infty} [a_l \cos(l\theta) + b_l \sin(l\theta)] r^l \\ \phi_{ext}(r, \theta) &= \frac{a'_0}{2} + \frac{c_0}{2} \ln r + \sum_{l=1}^{\infty} [c_l \cos(l\theta) + d_l \sin(l\theta)] r^{-l},\end{aligned}\tag{A17}$$

respectively for $0 \leq r \leq R$ and $r \geq R$. For a given boundary condition on the circle of radius R : $\phi(R, \theta) \equiv \phi_0(\theta)$, it is easy to obtain all coefficients as follows:

$$\begin{aligned}a_l &= \frac{1}{\pi R^l} \int_{-\pi}^{\pi} \phi_0(\theta') \cos(l\theta') d\theta' \\ b_l &= \frac{1}{\pi R^l} \int_{-\pi}^{\pi} \phi_0(\theta') \sin(l\theta') d\theta' \\ c_l &= \frac{R^l}{\pi} \int_{-\pi}^{\pi} \phi_0(\theta') \cos(l\theta') d\theta' \\ d_l &= \frac{R^l}{\pi} \int_{-\pi}^{\pi} \phi_0(\theta') \sin(l\theta') d\theta'\end{aligned}\tag{A18}$$

where these also include the a_0 and c_0 coefficients in Eq. (A17) (b_0 and d_0 are identically zero). The a'_0 coefficient is obtained instead by equating the $l = 0$ interior and exterior solutions in Eq. (A17) at the boundary $r = R$, namely $a'_0 + c_0 \ln R = a_0$, from which $\phi_{ext}^{l=0}(r, \theta) = \frac{a_0}{2} + \frac{c_0}{2} \ln\left(\frac{r}{R}\right)$. Inserting all these expressions into Eq. (A17) and using the identity $1 + 2 \sum_{l=1}^{\infty} x^l \cos(l\theta) = \frac{1-x^2}{x^2-2x \cos \theta + 1}$ ($0 \leq x < 1$) we can rewrite both interior and exterior solutions as power series or with Poisson integrals:

$$\begin{aligned}\phi_{int}(r, \theta) &= \frac{1}{2\pi} \int_{-\pi}^{\pi} \phi_0(\theta') d\theta' + \frac{1}{\pi} \sum_{l=1}^{\infty} \left[\int_{-\pi}^{\pi} \phi_0(\theta') \cos(l(\theta' - \theta)) d\theta' \right] \left(\frac{r}{R}\right)^l \\ &= \frac{1}{2\pi} \int_{-\pi}^{\pi} \phi_0(\theta') \frac{1 - \left(\frac{r}{R}\right)^2}{\left(\frac{r}{R}\right)^2 - 2\left(\frac{r}{R}\right) \cos(\theta' - \theta) + 1} d\theta' \\ \phi_{ext}(r, \theta) &= \frac{1}{2\pi} \int_{-\pi}^{\pi} \phi_0(\theta') d\theta' \left(1 + \ln\left(\frac{r}{R}\right)\right) + \frac{1}{\pi} \sum_{l=1}^{\infty} \left[\int_{-\pi}^{\pi} \phi_0(\theta') \cos(l(\theta' - \theta)) d\theta' \right] \left(\frac{R}{r}\right)^l \\ &= \frac{1}{2\pi} \int_{-\pi}^{\pi} \phi_0(\theta') \left[\ln\left(\frac{r}{R}\right) + \frac{1 - \left(\frac{R}{r}\right)^2}{\left(\frac{R}{r}\right)^2 - 2\left(\frac{R}{r}\right) \cos(\theta' - \theta) + 1} \right] d\theta'.\end{aligned}\tag{A19}$$

As it was done for the case $D \neq 2$, we can consider a single point mass at the origin in a $D = 2$ space as $\tilde{\rho}(\mathbf{r}) = \tilde{m}_{(2)} \delta^{(2)}(\mathbf{r})$. The spherical symmetry of $\phi_{ext}(r)$ obtained from the third line of Eq. (A19) requires $l = 0$

¹⁸ We still require the potential at the center to be non singular, but we will allow the potential at infinity to diverge at most logarithmically.

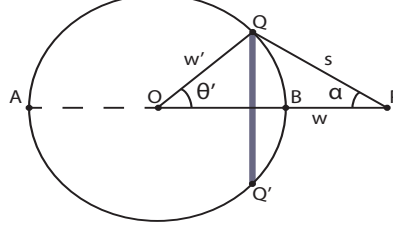


FIG. 4. General geometry used for spherical mass distributions.

and neglecting constant terms the potential simplifies as $\phi(r) = C \ln r$, where C is some constant to be determined. Following the procedure used for the $D \neq 2$ above, a direct computation gives $\nabla_{(2)}^2 \phi(r) = 2\pi C \delta^{(2)}(\mathbf{r})$ while the generalized Poisson equation (22) implies $\nabla_{(2)}^2 \phi(r) = 4\pi G \tilde{m}_{(2)} \delta^{(2)}(\mathbf{r})$. Comparing the two results, we determine the constant $C = 2G\tilde{m}_{(2)}$ and $\phi(r) = 2G\tilde{m}_{(2)} \ln r \rightarrow \frac{2G\tilde{m}_{(2)}}{l_0^2} \ln(r/l_0)$, including also the scale length l_0 for dimensional correctness. This result confirms the second line of our general equation (17) for the gravitational potential in the $D = 2$ case.

Appendix B: Spherically symmetric mass distributions

In this section we will consider the gravitational field $\mathbf{g}(w)$ due to a spherically symmetric source mass distribution $\tilde{\rho}(w')$, in a fractal space of dimension $D(w)$ also depending on the distance from the center of the coordinate system. We will expand and generalize the standard Newtonian derivation, based on the computation of the field due to an infinitesimal spherical shell (see for example [60], pp 223-225). Since the gravitational field can be computed directly from the mass distribution, following Eq. (14), we will not use the gravitational potential ϕ in this section.

The geometry is illustrated in Fig. 4. The distance s between the source point Q and the field point P is equivalent to the quantity $|\mathbf{w} - \mathbf{w}'|$ in Eq. (14), with $w^2 + w'^2 - 2ww' \cos \theta' = s^2$ due to the law of cosines and, by differentiating, $ww' \sin \theta' d\theta' = sds$. We also note that $\sin \theta' = \sqrt{1 - \cos^2 \theta'} = \sqrt{1 - \frac{(w^2 + w'^2 - s^2)^2}{4w^2 w'^2}}$ and that in the triangle OPQ we also have $\cos \alpha = \frac{s^2 + w^2 - w'^2}{2ws}$, which is useful to project the field into the radial direction OP . For a uniform spherical shell of radius w' and dimension $2 < D \leq 3$, the mass of the infinitesimal ring outlined in the figure between points Q and Q' is:

$$\begin{aligned} d\tilde{m}_{(D)} &= \frac{\pi^{\frac{D}{2}-1}}{\Gamma(\frac{D}{2}-1)} \tilde{\rho}(w') w'^{D-1} dw' |\sin \theta'|^{D-2} d\theta' \int_0^{2\pi} |\cos \varphi'|^{D-3} d\varphi' \\ &= \frac{2\pi^{\frac{D-1}{2}}}{\Gamma(\frac{D-1}{2})} \tilde{\rho}(w') w'^{D-1} dw' |\sin \theta'|^{D-2} d\theta'. \end{aligned} \quad (B1)$$

The previous equation follows from Eq. (15) expressed in terms of spherical coordinates, as discussed in Sect. III. Following Eq. (14), we can obtain the infinitesimal contribution to the field at point P , due to the whole spherical shell, by integrating over the angle θ' :

$$\begin{aligned} d\mathbf{g}(w) &= -\frac{4\sqrt{\pi}G}{l_0^2} \frac{\Gamma(D/2)}{\Gamma(\frac{D-1}{2})} \tilde{\rho}(w') w'^{D-1} dw' \int_0^\pi |\sin \theta'|^{D-2} \frac{1}{s^{D-1}} \frac{s^2 + w^2 - w'^2}{2ws} d\theta' \hat{\mathbf{w}} \\ &= -\frac{4\sqrt{\pi}G}{l_0^2} \frac{\Gamma(D/2)}{\Gamma(\frac{D-1}{2})} \frac{\tilde{\rho}(w') w' dw'}{2^{D-2} w^{D-1}} \int_{w-w'}^{w+w'} [(2w'w)^2 - (w^2 + w'^2 - s^2)^2]^{\frac{D-3}{2}} \left(\frac{s^2 + w^2 - w'^2}{s^{D-1}} \right) ds \hat{\mathbf{w}} \\ &= -\frac{4\pi G}{l_0^2 w^{D-1}} \tilde{\rho}(w') w'^{D-1} dw' \hat{\mathbf{w}}. \end{aligned} \quad (B2)$$

Due to the symmetry, in this equation we considered just the radial components of the field at point P , while the sum of the perpendicular components vanishes, and we used all the relations mentioned above to express the various quantities in terms of the variable s . The angular integration over θ' was then transformed into an integration over s , by assuming $w > w'$ and the integral in the second line of Eq. (B2) is: $\int_{w-w'}^{w+w'} \left[(2w'w)^2 - (w^2 + w'^2 - s^2)^2 \right]^{\frac{D-3}{2}} \left(\frac{s^2 + w^2 - w'^2}{s^{D-1}} \right) ds = \frac{2^{D-2} \Gamma(1 - \frac{D}{2}) \Gamma(\frac{D-1}{2}) \sin(\frac{D\pi}{2}) w'^{D-2}}{\sqrt{\pi}}$, which yields the simplified result on the third line of the last equation, in terms of the radial unit vector $\hat{\mathbf{w}}$.

The total field $\mathbf{g}(w)$ at point P can then be obtained with a further integration over all the “inner” spherical shells ($0 < w' < w$) noting that the dimension D should also be considered as a function of the field point radius w , i.e. $D = D(w)$, therefore:

$$\mathbf{g}(w) = -\frac{4\pi G}{l_0^2 w^{D(w)-1}} \int_0^w \tilde{\rho}(w') w'^{D(w)-1} dw' \hat{\mathbf{w}}. \quad (B3)$$

The standard Newtonian result $\mathbf{g}(w) = -\frac{4\pi G}{l_0^2 w^2} \int_0^w \tilde{\rho}(w') w'^2 dw' \hat{\mathbf{w}}$ is recovered from the previous equation in the case of a constant dimension $D = 3$. We should also remark that, as in the standard Newtonian case, all contributions to the field $\mathbf{g}(w)$ due to the “outer” spherical shells, that is for $w' > w > 0$, are identically zero also in the case of variable dimension $D(w)$. In fact, for the outer shells the integral in the second line of Eq. (B2) would only differ by the lower limit: $w' - w$, instead of $w - w'$. It is easy to check that $\int_{w'-w}^{w+w'} \left[(2w'w)^2 - (w^2 + w'^2 - s^2)^2 \right]^{\frac{D-3}{2}} \left(\frac{s^2 + w^2 - w'^2}{s^{D-1}} \right) ds = 0$ and, therefore, outer spherical shells do not contribute to the field. Newton’s first theorem for a spherical distribution of matter, namely that *a body inside a spherical shell of matter experiences no net gravitational force from that shell*, still holds.

The main result in Eq. (B3) was derived for the case $2 < D \leq 3$, but it is easy to check that this result is actually valid for the whole range $1 \leq D \leq 3$. The special case $D = 2$ involves a “circular” distribution of matter, over the circle of radius w' in Fig. 1. In this case, the “ring” reduces to the two symmetric points Q and Q' , with the infinitesimal “ring” mass $d\tilde{m}_{(D)} = 2\tilde{\rho}(w')w'dw'd\theta'$, where the factor of 2 accounts for the two equal contributions from points Q and Q' , while the θ' integration is between 0 and π . In this way, the derivation is similar to the one outlined above and Eq. (B3) still holds. In particular, for a space of constant $D = 2$, we have $\mathbf{g}(w) = -\frac{4\pi G}{l_0^2 w} \int_0^w \tilde{\rho}(w')w'dw' \hat{\mathbf{w}}$.

The case $1 < D < 2$ would still be related to a “circular” distribution of matter, but with the infinitesimal mass contribution given by $d\tilde{m}_{(D)} = 2\frac{\pi^{\frac{D-1}{2}}}{\Gamma(\frac{D-1}{2})} \tilde{\rho}(w')w'^{D-1}dw' |\sin\theta'|^{D-2} d\theta'$, which is equivalent to the result in the second line of Eq. (B1). Therefore, the general result in Eq. (B3) also follows in this case.

For $D = 1$, the “spherical” distribution of matter reduces just to points A and B in the figure. The infinitesimal mass is simply $d\tilde{m}_{(D)} = 2\tilde{\rho}(w')dw'$ and, for a constant $D = 1$ space, we have $\mathbf{g}(w) = -\frac{4\pi G}{l_0^2} \int_0^w \tilde{\rho}(w')dw' \hat{\mathbf{w}}$. In all these cases, it is easy to prove that “outer” shells do not contribute to the field and Newton’s first theorem still holds.

Finally, it is interesting to consider also $0 < D < 1$. In this case, $d\tilde{m}_{(D)} = 2\frac{\pi^{D/2}}{\Gamma(D/2)} \tilde{\rho}(w')w'^{D-1}dw'$, which yields an infinitesimal contribution to the field at P , due to source points A and B , as $d\mathbf{g}(w) = -\frac{4\pi G}{l_0^2} \tilde{\rho}(w) \frac{w'^{D-1}}{|w-w'|^{D-1}} dw' \hat{\mathbf{w}}$, following directly Eq. (14). In this case the overall field at point P is due to both inner and outer contributions:

$$\mathbf{g}(w) = -\frac{4\pi G}{l_0^2} \left[\int_0^w \tilde{\rho}(w') \frac{w'^{D(w)-1}}{(w-w')^{D(w)-1}} dw' + \int_w^\infty \tilde{\rho}(w') \frac{w'^{D(w)-1}}{(w'-w)^{D(w)-1}} dw' \right] \hat{\mathbf{w}}, \quad (B4)$$

since, in general, the second integral in Eq. (B4) is not equal to zero.

- [1] K. B. Oldham and J. Spanier, *The fractional calculus* (Academic Press [A subsidiary of Harcourt Brace Jovanovich, Publishers], New York-London, 1974) pp. xiii+234, theory and applications of differentiation and integration to arbitrary order, with an annotated chronological bibliography by Bertram Ross, Mathematics in Science and Engineering, Vol. 111.
- [2] K. S. Miller and B. Ross, *An introduction to the fractional calculus and fractional differential equations*, A Wiley-Interscience Publication (John Wiley & Sons, Inc., New York, 1993) pp. xvi+366.
- [3] I. Podlubny, *Fractional differential equations*, Mathematics in Science and Engineering, Vol. 198 (Academic Press, Inc., San Diego, CA, 1999) pp. xxiv+340, an introduction to fractional derivatives, fractional differential equations, to methods of their solution and some of their applications.

[4] R. Herrmann, *Fractional calculus: An introduction for physicists* (World Scientific, Hackensack, USA, 2011) p. 261.

[5] R. Hilfer, ed., *Applications of fractional calculus in physics* (World Scientific Publishing Co., Inc., River Edge, NJ, 2000) pp. viii+463.

[6] V. Tarasov, *Fractional Dynamics: Application of Fractional Calculus to Dynamics of Particles, Fields and Media* (2011).

[7] M. Zubair, M. Mughal, and Q. Naqvi, *Electromagnetic Fields and Waves in Fractional Dimensional Space* (2012).

[8] Yu. Baryshev and P. Teerikorpi, *Discovery of cosmic fractals* (River Edge, USA: World Scientific (2002) 373 p, 2002).

[9] L. Nottale, *Scale relativity and fractal space-time* (London, UK: Imp. Coll. Pr. (2011) 742 p, 2011).

[10] M. Milgrom, *Astrophys. J.* **270**, 365 (1983).

[11] M. Milgrom, *Astrophys. J.* **270**, 371 (1983).

[12] M. Milgrom, *Astrophys. J.* **270**, 384 (1983).

[13] J. D. Bekenstein, *Phys. Rev. D* **70**, 083509 (2004), [Erratum: *Phys. Rev.D* **71**, 069901(2005)], arXiv:0403694 [astro-ph].

[14] R. H. Sanders, *Mon. Not. Roy. Astron. Soc.* **363**, 459 (2005), arXiv:0502222 [astro-ph].

[15] S. McGaugh, F. Lelli, and J. Schombert, *Phys. Rev. Lett.* **117**, 201101 (2016), arXiv:1609.05917 [astro-ph.GA].

[16] F. Lelli, S. S. McGaugh, J. M. Schombert, and M. S. Pawlowski, *Astrophys. J.* **836**, 152 (2017), arXiv:1610.08981 [astro-ph.GA].

[17] J. Bekenstein and M. Milgrom, *Astrophys. J.* **286**, 7 (1984).

[18] M. Milgrom, *Astrophys. J.* **287**, 571 (1984).

[19] S. McGaugh, *Astrophys. J.* **683**, 137 (2008), arXiv:0804.1314 [astro-ph].

[20] M. Milgrom, *Acta Phys. Polon.* **B32**, 3613 (2001), arXiv:0112069 [astro-ph].

[21] J. D. Bekenstein, *Contemp. Phys.* **47**, 387 (2006), arXiv:0701848 [astro-ph].

[22] B. Famaey and S. McGaugh, *Living Rev. Rel.* **15**, 10 (2012), arXiv:1112.3960 [astro-ph.CO].

[23] M. Milgrom, *Annals Phys.* **229**, 384 (1994), arXiv:9303012 [astro-ph].

[24] M. Milgrom, *Phys. Lett.* **A253**, 273 (1999), arXiv:9805346 [astro-ph].

[25] S. S. McGaugh, *Galaxies* **2**, 601 (2014), arXiv:1412.3767 [astro-ph.GA].

[26] R. B. Tully and J. R. Fisher, *Astron. Astrophys.* **54**, 661 (1977).

[27] F. Lelli, S. S. McGaugh, and J. M. Schombert, *Astrophys. J.* **816**, L14 (2016), arXiv:1512.04543 [astro-ph.GA].

[28] F. Lelli, S. S. McGaugh, J. M. Schombert, H. Desmond, and H. Katz, *Mon. Not. Roy. Astron. Soc.* **484**, 3267 (2019), arXiv:1901.05966 [astro-ph.GA].

[29] R. Sancisi, *Proceedings, IAU Symposium 220: Dark Matter in Galaxies: Sydney, Australia, July 21-25, 2003*, (2003), [IAU Symp.220,233(2004)], arXiv:0311348 [astro-ph].

[30] F. Lelli, S. S. McGaugh, and J. M. Schombert, *Astron. J.* **152**, 157 (2016), arXiv:1606.09251 [astro-ph.GA].

[31] P. Li, F. Lelli, S. McGaugh, and J. Schombert, *Astron. Astrophys.* **615**, A3 (2018), arXiv:1803.00022 [astro-ph.GA].

[32] J. P. Ostriker and P. J. Steinhardt, *Nature* **377**, 600 (1995).

[33] D. Boito, L. N. S. de Andrade, G. de Sousa, R. Gama, and C. Y. M. London, (2018), arXiv:1809.07368 [physics.class-ph].

[34] K. T. McDonald, (2019), <http://www.physics.princeton.edu/~mcdonald/examples/2dem.pdf>:unpublished.

[35] P. Ehrenfest, *Annalen der Physik* **366**, 440 (1920), <https://onlinelibrary.wiley.com/doi/pdf/10.1002/andp.19203660503>.

[36] C. Callender, *Studies in the History and Philosophy of Modern Physics* **36**, 113 (2005).

[37] I. R. Lapidus, *American Journal of Physics* **49**, 807 (1981).

[38] I. R. Lapidus, *American Journal of Physics* **50**, 155 (1982).

[39] F. J. Asturias and S. R. Aragón, *American Journal of Physics* **53**, 893 (1985).

[40] L. B. Castro and A. S. de Castro, *Electron. J. Theor. Phys.* **7**, 155 (2010), arXiv:1003.2993 [quant-ph].

[41] M. E. Peskin and D. V. Schroeder, *An Introduction to Quantum Field Theory*, by Michael Edward Peskin and Daniel V. Schroeder. ISBN 13 978-0-201-50397-5, ISBN-10 0-201-50397-2. Published by Westview Press, Perseus Books Group, 1995. (1995).

[42] C. G. Bollini and J. J. Giambiagi, *Nuovo Cim.* **B12**, 20 (1972).

[43] G. 't Hooft and M. J. G. Veltman, *Nucl. Phys.* **B44**, 189 (1972).

[44] K. G. Wilson, *Phys. Rev. D* **7**, 2911 (1973).

[45] K. Svozil, *Journal of Physics A Mathematical General* **20**, 3861 (1987).

[46] G. U. Varieschi, *Journal of Applied Mathematics and Physics* **6**, 1247 (2018), arXiv:1712.03473 [physics.class-ph].

[47] V. E. Tarasov, *J. Math. Phys.* **55**, 083510 (2014), arXiv:1503.02392 [math-ph].

[48] V. E. Tarasov, *Communications in Nonlinear Science and Numerical Simulation* **20**, 360 (2015).

[49] F. H. Stillinger, *Journal of Mathematical Physics* **18**, 1224 (1977), <https://doi.org/10.1063/1.523395>.

[50] C. Palmer and P. N. Stavrinou, *Journal of Physics A: Mathematical and General* **37**, 6987 (2004).

[51] J. Binney and S. Tremaine, *Galactic Dynamics: Second Edition*, by James Binney and Scott Tremaine. ISBN 978-0-691-13026-2 (HB). Published by Princeton University Press, Princeton, NJ USA, 2008. (2008).

[52] G. U. Varieschi, in progress (2020).

[53] S. I. Muslih, D. Baleanu, and E. M. Rabei, *Central European Journal of Physics* **5**, 285 (2007).

[54] A. A. Rousan, E. Malkawi, E. M. Rabei, and H. Widyan, *Frac. Calc. Appl. Anal.* **5**, 155 (2002).

[55] A. Giusti, (2020), arXiv:2002.07133 [gr-qc].

[56] DLMF, *NIST Digital Library of Mathematical Functions*, <http://dlmf.nist.gov/>, Release 1.0.25 of 2019-12-15, f. W. J. Olver, A. B. Olde Daalhuis, D. W. Lozier, B. I. Schneider, R. F. Boisvert, C. W. Clark, B. R. Miller, B. V. Saunders, H. S. Cohl, and M. A. McClain, eds.

[57] I. S. Gradshteyn, I. M. Ryzhik, A. Jeffrey, and D. Zwillinger, *Table of Integrals, Series, and Products* (2007).

[58] P. Morse and H. Feshbach, *Methods of theoretical physics*, International series in pure and applied physics (McGraw-Hill,

1953).

- [59] V. Smirnov and A. Lohwater, *A Course of Higher Mathematics: Adiwes International Series in Mathematics*, v. 2 (Elsevier Science, 2014).
- [60] G. Fowles and G. Cassiday, *Analytical mechanics* (Thomson Brooks/Cole, 2005).